LINDA HALL LIBRARY
5109 CHERRY STREET
KANSAS CITY, MISSOURI
64110-2498
PHONE (816) 363-4600
FAX: (816) 926-8785

4/6/01 DocServ #: 17082 (57)

Shelved as: TC 1505 .I58 1994 199-255

Location:

SHIP TO:

Attn: Sheila McNary
Massachusetts Institute of Technology
77 Massachusetts Avenue - Room 5-222
Cambridge MA -2139
USA

Fax: 617 253 8125
Phone: 617 253 9713
Ariel:
Email: mcnary@mit.edu

Title: Offshore Technology, ASME OMAE 1994

Volume: 1

Issue:

Date:

Author: Michael S. Pantazopoulos

Article Title: Vortex-Induced Vibration Parameters: Critical Review

Pages:

Accept Non English? No

Regular
-email-
LHL

This request complies with "Fair Use"

Max Cost:

Reference Number:

Account Number:
FEDEX Account Number: 1487 1056 2

Notes: Originally requested by email? not found
3/16/01 – no acknowledgement received

DOCSERV / WEB / PULL SLIP

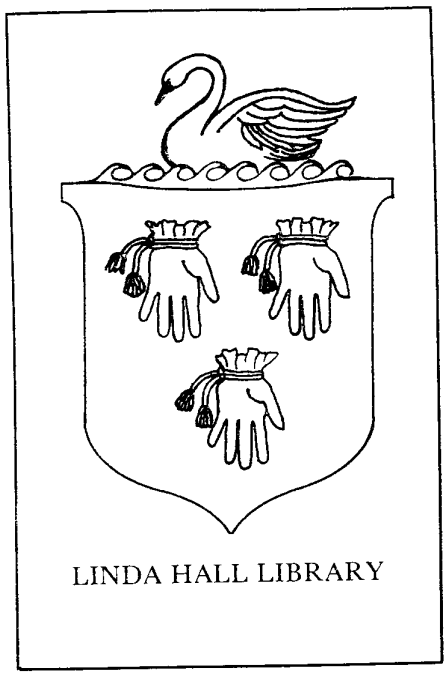

ISBN No. 0-7918-1264-2

Library of Congress Catalog Number 82-70515

1994 OMAE – Volume I, Offshore Technology
ASME 1994

VORTEX-INDUCED VIBRATION PARAMETERS: CRITICAL REVIEW

Michael S. Pantazopoulos
Offshore Division
Exxon Production Research Company
Houston, Texas

ABSTRACT

This paper presents the results of a research study to develop an empirical basis for modeling hydrodynamic vortex-induced vibrations in marine risers, tethers, and other slender marine structures. Published model tests were reviewed, and evaluated, including more than 150 model tests compiled to provide extensive insight and understanding of the hydrodynamic VIV parameters. The data could provide values for the VIV parameters used in a VIV analysis model. The most important VIV parmeters are: the lift coefficient, the shedding frequency (Strouhal number), the correlation length, and the shedding frequency bandwidth.

The empirical data are based on steady flow model tests that are applicable to long, flexible cylinders simulating marine risers undergoing large amplitude vibrations of the order of up to one riser diameter. The empirical data account for the lock-in phenomenon that is the most important consideration to predict accurately VIV extreme response.

Conclusions and recommendations are included to develop an empirical methodology that captures the hydrodynamic VIV phenomena. These recommendations provide the basis for the development of a VIV prediction model that is a significant extention from previous models in the literature, because it can predict lock-in behavior of a flexible cylinder in shear flow.

1.0 INTRODUCTION

Many types of marine structures in the offshore industry have been affected by vortex-excited vibrations. These include risers, tethers, and conductor tubes employed in oil drilling and production for exploratory drilling and floating production, pipelines, and members of jacketed structures. Deep water pile installation and driving operations also are susceptible to problems arising from vortex shedding. Several case studies of fatigue damage of marine structures due to VIV have been documented in the open literature [Every et. al. (1980), Lewis et. al. (1990), etc.].

Suppression devices have been used sometimes to eliminate or reduce the VIV response and prevent fatigue damage. Strakes and fairings are two of the most commonly used devices. However, extensive model tests at high cost are necessary to design these suppression devices for a particular application. In 1980, Exxon fitted its drilling riser with adjustable fairings and its casing with strakes to complete drilling on its acreage in the Guiana current off Brazil [Gardner (1982)].

More recently, in August 1989, the Loop Current moved into the northern Gulf of Mexico, severely affecting exploration drilling in several lease block areas. At least six operators were forced to shut down operations. The affected blocks were primarily in deep water; however, strong currents were found at sites with water depths as shallow as 450 ft.

Developing the technology for estimating VIV response is a critical need for fatigue design of drilling and production risers in TLP and FPS riser systems. The need for a complimentary analysis/design capability to predict when a problem will occur has been recognized by the industry since the early 60's. Since then, vortex-induced vibrations of slender cylinders has become one of the most extensively researched topics in the hydrodynamics and mechanics literature. However, the complexity of the problem does not lend itself to standard analytical or numerical solutions. Many research efforts have raised

more questions than they answered. Dozens of approximate methods have been proposed to model specific aspects of VIV response, but none have been widely accepted for design purposes. Numerous model tests have been conducted to investigate a particular aspect of the problem or to satisfy the needs of a specific numerical or analytical model. Much of this testing was conducted with the objective of establishing empirical coefficients under a fairly narrow range of conditions. Experiment design, experimental techniques, methods for data reduction, details of the reported results, and even the terminology vary widely between references.

The weakness in the analysis/design capabilities to predict VIV of marine structures was recognized in the 80's when high current became a problem in exploratory drilling and production. In the late 80's, VIV research was culminated in MIT's SHEAR program, which was a random vibration model for strictly multiple mode, broad-band random response combined with a dynamic solution method for cables and risers in shear flow [Vandiver, et. al. (1988)]. SHEAR was developed as part of a JIP at MIT by Prof. K. Vandiver, and is generally considered the state-of-the-art. However, after several years of development through the ongoing JIP, the latest version of SHEAR is still uncalibrated, and further work is needed before it is directly useful in industry applications.

Exxon Production Research Co. (EPR) has recognized the complexity and importance of the VIV phenomenon in drilling and production operations and has devoted a substantial amount of resources towards understanding it in the last ten years. A number of fundamental model tests at BHRA, and at Western Ontario University [Vickery et. al. (1983)] were performed that assisted in the basic understanding of the phenomenon. Overall, these efforts were focused on model and field tests and VIV prediction capabilities were based on typical simplified models (reduced velocity checks), derived from experiments, and did not address the nonlinear fluid-structure interaction between the fluid forces and the complex structural response of risers in deepwater.

In 1990 EPR developed a basic analytical method to predict VIV response of risers for narrow- (lock-in) and broad-band (strumming) response. This model is designed to enable prediction of lock-in behavior of a flexible cylinder in shear flow.

Specifically, EPR's basic approach to modeling vortex-induced vibrations is to empirically model the hydrodynamic forcing function for a short segment of an oscillating cylinder, empirically model correlation between forces at different locations, and represent structural mass and stiffness with standard finite elements. Equations of motion can then be developed and solved iteratively in the frequency domain, with various parameters depending on flow characteristics, response frequency, and response amplitude.

The key advantage to this approach is the ability to calibrate the local hydrodynamic model to existing data in the literature, specifically spring-mounted rigid cylinder data. To this end, extensive compilation of model test results was necessary to identify qualitative and quantitative characteristics of the parameters used in our VIV program.

2.0 OBJECTIVES

The overall goal of a VIV analysis effort is to develop a general VIV analysis procedure capable of representing the wide range of vibration behavior associated with long, flexible cylinders in shear current. A suitable strategy is to utilize familiar, detailed methods of analysis for parts of the problem which are well known (e.g. structural response to a given load), and calibrate simple empirical models for the complex hydrodynamic loadings which arise from the vortex shedding process (the local hydrodynamic load).

One approach to utilize data from rigid cylinder lab tests to model the local hydrodynamic load is based on the philosophy that short elements of a long flexible cylinder may be modeled as a rigid cylinder. The challenge is the accurate modeling of the hydrodynamic interaction and response coupling of the small elements that form the flexible cylinder (marine riser). This approach must be continually evolving as new test data and developments in VIV become available.

Modeling VIV riser behavior is dependent on a number of empirical parameters such as Strouhal number, correlation length and lift coefficient. These parameters are dependent on other flow parameters such as Reynolds number, surface roughness, Keulegan-Carpenter number, and turbulence intensity. No single test can provide measurements and data for all the parameters involved in VIV. Most of the tests provide data for a few parameters (lift coefficient and Strouhal number are the most common), disregarding the effect of the others. Selection, interpretation, and integration of test data is critical to model VIV of marine risers.

The objective of this study is to integrate key points selected and interpreted from the open literature into a consistent framework for developing an empirical model for the hydrodynamic forces associated with vortex-induced vibrations of marine risers.

Recommendations in this paper are based on an extensive literature review, including more than 200 references, laboratory and test data for use in the calibration of a VIV methodology. The compiled data include hydrodynamic coefficients as a function of flow parameters and response characteristics.

Specifications of this work are as follows:

- More than 150 test data were selected from the studies of other researchers. EPR did not conduct new experiments to study the effect of VIV parameters on cylinder response as part of this project.

- The focus was on long, flexible cylinders (e.g. marine risers) in the marine environment (water). Flexible cylinders have natural frequencies within the range of expected vortex shedding frequencies.

- The primary concern was large amplitude response (0.2-1 D, D=riser diameter) associated with rapid accumulation of fatigue. VIV amplitudes greater than 1D have very rarely been reported in field test observations of risers, casing, and pipes.

- The report covers steady flow only (current, primarily shear). Separate research is needed to identify the effect of waves on VIV response as several researchers have recently indicated [Bearman (1991)].

Although data has been collected from many sources concerning VIV response, there is still a shortage of data for certain parameters. There is very limited data describing the effect of turbulence intensity and surface roughness on force and response parameters in VIV riser analysis. The search for new model test data and maintenance of a parameter database will be essential for continued improvement of the VIV analysis.

3.0 MODEL TEST DATA

The most essential element of utilizing data from the literature is a thorough understanding of all issues that can significantly affect test results. First, experiments are based on a variety of assumptions and simplifications that may limit the applicability of the results. Such assumptions and simplifications are not always explicitly stated in the published work. Second, inconsistencies arise that are the product of the researcher's implicit focus on one aspect of a very complicated problem. For instance, a test may be designed with the emphasis on fundamental hydrodynamics of the flow, and therefore details essential to the dynamic behavior of the mechanical system may be omitted or inaccurate. Third, inconsistent use of terminology is found throughout the literature. For example, what some researchers report as lift force from oscillating cylinder tests often includes damping or added mass forces. Finally, published test results must be viewed in the context of several more general issues, such as Reynolds number, end effects, instrumentation design, and motion of the test cylinder (fixed vs. self-excited vs. forced-displacement).

The above discussion is by no means comprehensive, but it helps to illustrate the difficulties inherent to compiling and using data from the open literature. However, the investment in these data is so large, and the fundamental problem is so complex, that there is a great deal of incentive to derive the maximum benefit out of existing data instead of performing further tests. Subsequent sections of this paper attempt to present compilations of these data to facilitate their use in a variety of VIV response models. To assist the reader in interpreting these data, specific issues relevant to particular data are discussed in detail along with plots of the compiled data. The objective of this section is to provide an overview of model testing as typically found in the literature, and discuss several significant issues that should be understood in order to make effective use of any data compiled from published test results.

In general, the majority of VIV model tests have been performed in a wind tunnel at subcritical Reynolds numbers. Most model test cylinders were smooth (surface roughness less than $2x10^{-5}$) with constant diameter and uniform velocity profiles. Few tests with sheared flow conditions have been published. Most researchers attempt to minimize end effects by providing end plates on the cylinder, although some data are taken from short segments near the center of a very long cylinder. A variety of measurements are reported, including total force, displacement, and pressure. Test specimens included cantilever beams, beams with pinned or fixed ends, and rigid beams mounted on springs. A single stationary vertical or horizontal cylinder was used in the majority of the tests. Fewer tests have used displacement-controlled, oscillated cylinders.

3.1 Reynolds Number

The flow pattern around a circular cylinder can generally be characterized by the Reynolds number of the incident flow and by the location of points at which the flow separates from the cylinder surface, which in turn depend on the state of the boundary layer (laminar or turbulent).

The major Reynolds number regimes of vortex shedding from a smooth circular cylinder in uniform flow are given in Figure 3.1. The Reynolds number range $300<Re<1.5x10^5$ is called subcritical. In this range, the laminar boundary layers separate at about 80 degrees aft of the nose of the cylinder and vortex shedding is strong and periodic.

The range $1.5x10^5<Re<3.5x10^6$, referred to in the literature as the transitional region, includes the critical region ($1.5x10^5<Re<3.5x10^5$) and the supercritical region ($3.5x10^5<Re<3.5x10^6$). In these regions, the cylinder boundary layer becomes turbulent, the separation points move aft to 140 degrees, and the cylinder drag coefficient drops abruptly. Laminar separation bubbles and three-dimensional effects disrupt the regular shedding process and broaden the spectrum of shedding frequencies for smooth surface cylinders [Bearman (1969)].

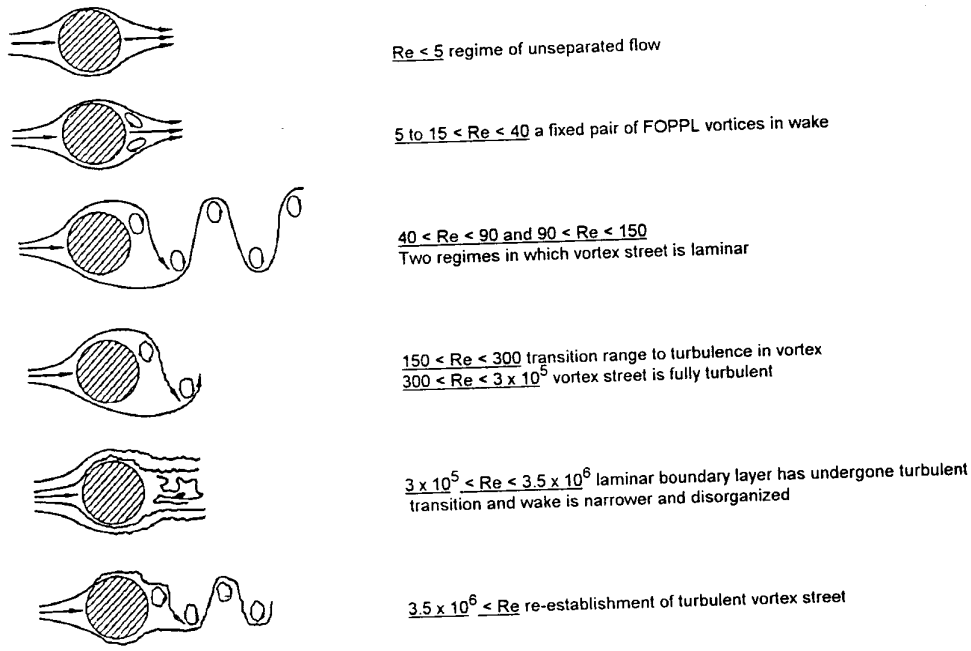

FIGURE 3.1 REYNOLDS NUMBER REGIMES (LIENHARD 1966)

In the postcritical Reynolds number range ($Re>3.5x10^6$), regular vortex shedding is re-established with a turbulent cylinder boundary layer. The vortex shedding persists at Reynolds numbers as high as 10^{11} [Griffin et. al. (1982)].

Many engineering applications for VIV analysis are in the upper subcritical and transitional Reynolds number ranges. For example, the Reynolds number for a North Sea TLP production riser in a 1-knot current is $7.5x10^4$, while for a GOM drilling riser with buoyancy in a 4-knot current the Reynolds number is $2.4x10^6$. Unfortunately, the majority of model tests are performed at subcritical Reynolds numbers. This is partly due to the stable, well-defined character of the flow in this region. The tests are easier to perform, and the results are more readily interpreted. Also, especially at transitional Reynolds numbers, sensitivity of the flow to even the smallest perturbations caused by the test conditions is very high [Schewe (1983)]. In addition, existing model test facilities and the attainable speed for carriage equipment and/or current circulation equipment limits most model tests to lower Reynolds number regions. Nevertheless, a number of researchers have performed tests in the transitional and postcritical flow regions. Therefore there is some data that can be used for engineering models of VIV at higher Reynolds numbers. These data are also useful for checking conclusions based on data from subcritical Reynolds numbers.

Finally, note that Reynolds number alone is only a general guide to the flow regime. Other factors, such as roughness of the cylinder surface and turbulence of the incident flow, significantly affect the flow. For example, the changes in flow character described above for a smooth cylinder in the transition region can occur at substantially lower Reynolds numbers for a roughened cylinder. Therefore, many engineering problems occurring in upper subcritical or transitional Reynolds numbers are actually characterized by postcritical flow.

3.2 End Effects

Another problem with model test data often arises due to the presence of three-dimensional flow conditions, otherwise known as end effects. Many experiments have shown that disturbances in the flow along the cylinder due to the proximity of the cylinder ends, the free surface, or test tank walls can have a significant effect on test results. Two methods have been used to ensure two-dimensional flow conditions: 1) providing sufficiently long cylinders (where the force/pressure measurements are taken far from the ends), and 2) the addition of end plates to suppress the wrapping of vortices along the cylinder length.

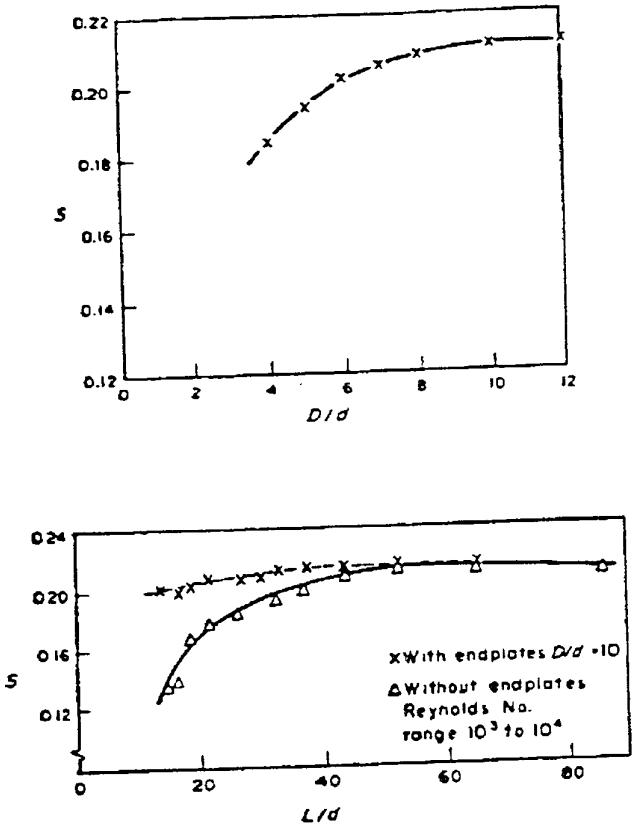

$\frac{D}{d}$ = end plate aspect ratio

$\frac{L}{d}$ = aspect ratio

L = length

d = diameter

S = Strouhal number

FIGURE 3.2 END EFFECTS ON VORTEX SHEDDING FREQUENCY (GOUDA 1975)

Gouda (1975) presented the results of wind tunnel tests with cylinders of varying length, with and without end plates. The variation of vortex shedding frequency with cylinder length is illustrated in Figure 3.2. Shedding frequency is consistently lower for cylinders with three-dimensional flow effects than for cylinders with end plates except for L/D>50; for cylinders of L/D=15 the shedding frequency is 35% lower than for the infinite cylinder case. He proposed an aspect ratio of L/D=45 for no end effects without end plates. Griffin (1985) suggested conducting experiments with cylinders of sufficient length to minimize the effects of the end boundaries (length/diameter, L/D=100-120).

Gouda also investigated the effects of end plate size on vortex shedding frequency and showed that for a cylinder of L/D=18, the diameter of the end plates should be at least 10D (D=cylinder diameter) to avoid all end effects. Other researchers have suggested end plate diameters between 5D - 8D [Zdravkovich et. al. (1989), Farell et. al. (1988), Stansby (1974)]. These results illustrate the importance of end effects, and indicate that steps taken to mitigate end effects for any particular experiment should be understood when using the compiled data.

3.3 Instrumentation Design

Several methods have been used to take measurements in VIV model tests. Strain, force, and pressure gages are the most commonly used devices for measuring forces. Strain gages measure the deformation of the section, which is then used to calculate the force which caused it. Force gages (load cells) directly measure the total force on a cylinder section. Pressure gages measure the pressure at a point in the flow field. A combination of pressure gages placed around the cylinder circumference provides the pressure distribution, which can be integrated to calculate the local force.

When interpreting total force measurements, one has to bear in mind that hydrodynamic forces include possible spatial variations in local force. For example, the lift force across an instrumented test section may be less than perfectly correlated. The measured total force is reduced

by the lack of correlation, and therefore using the measured force divided by the section length would understate the actual lift force per unit length. In addition, forces and strains measured on moving cylinders include inertia effects that must be taken into account when the local hydrodynamic forces are sought.

For example, one particular set of oscillated cylinder experiments measured reaction force at one end of the test cylinder, which was mounted at both ends to a test frame [Gopalkrishnan (1993)]. Data reduction was carried out by assuming a uniform distributed load and simply-supported beam behavior. While this may in fact be true for much of the oscillated data, it clearly was not true for some of the stationary cylinder measurements, and probably contributed to the large scatter observed in the stationary lift coefficient.

A thorough discussion about correlation and inertia effects on the local forces is given by Howell and Novak (1980). They measured the total force on the cylinder by using a strain gage bridge on support arms of a spring-mounted rigid cylinder. When the cylinder oscillated, the strain gage recorded the sum of inertia forces and hydrodynamic forces. In order to minimize inertia forces on the model, the cylinder was made out of a thin veneer of birch over balsa diaphragms. In addition, force coefficients were corrected for correlation effects, which altered lift force estimates by 15-20%. This work demonstrates the importance of careful interpretation of test measurements with respect to the desired physical quantities.

3.4 Test Cylinder Motion

The type of model test performed is usually determined based on the specific test objectives (e.g. estimation of force coefficients, or establishing conditions under which large vibrations occur). Many tests conducted to estimate force coefficients were conducted with stationary cylinders instrumented to measure pressure or total force. Tests to investigate dynamic behavior were typically conducted on spring-mounted, rigid cylinders under uniform flow or on long, flexible cylinders under flow conditions ranging from uniform to highly sheared. Forced oscillation tests, in which the amplitude and frequency of cylinder motion is controlled, have been used to investigate hydrodynamic interaction (i.e. the effect of cylinder motion on hydrodynamic force). Most researchers are somewhat vague about their specific test objectives, and many fail to clearly distinguish between hydrodynamic interaction (added mass, damping) at cylinder oscillation frequencies and lift force at shedding frequencies.

3.4.1 Stationary Cylinders

Stationary cylinders in steady uniform flow have been studied extensively. Time-dependent forces occur on the cylinder and are typically measured and reported as functions of Reynolds number and other pertinent variables. Force measurements show that the inline (drag) force is quite regular, while the transverse force (lift) exhibits randomness. A great deal of the present literature documents drag and lift force coefficients based on stationary cylinder experiments. Use of these data for predicting motion requires an assumption commonly known as the quasi-steady flow assumption. The quasi-steady assumption essentially says that static fluid forces measured on a stationary body can be used to approximate dynamic fluid forces on an oscillating body.

This assumption is commonly accepted at reduced velocities (fluid velocity divided by the product of oscillation frequency and cylinder diameter) above ten [Blevins (1977)]. However, many VIV problems are concerned with reduced velocities below ten, and peak displacements often occur at reduced velocities between four and six. Therefore, a great deal of caution must be exercised when using results of stationary cylinder experiments to represent forces on oscillating cylinders at reduced velocities typical of VIV response. Hydrodynamic interaction may be minimal at very small oscillation amplitudes, but can be very significant at larger amplitudes. Clearly, the drawback to stationary cylinder experiments is that hydrodynamic interaction is completely neglected, yet it is of utmost importance for most practical offshore engineering applications.

3.4.2 Spring-Mounted Rigid Cylinders

Experiments with spring-mounted rigid cylinders have been performed using short, rigid cylinder segments. Feng (1968) demonstrated that the flow around a freely vibrating bluff body can change very rapidly with changes in reduced velocity. Since varying the reduced velocity also changes the amplitude ratio, it can be very difficult to determine the relative importance of these two effects on the resulting flow field. Furthermore, many real structures have more complicated dynamic behavior than simple spring-mounted rigid cylinders.

Chryssostomidis and Patrikalakis (1984) argued that spring-mounted rigid cylinder data may be used in VIV predictions of flexible structures under the following conditions:

1) Any force component measured in a rigid cylinder experiment which will make a flexible cylinder respond differently than the one used to conduct the rigid cylinder experiment must be neglected, and

2) The spanwise correlation of local hydrodynamic forces measured in a rigid cylinder experiment cannot model the effect of relative motion between different sections of a flexible cylinder.

Use of results from spring-mounted rigid cylinder tests in the prediction of vibrations of a flexible system also requires approximating response of the flexible system by

a small number of degrees of freedom. According to Chryssostomidis et. al. (1984), the need to represent the response of a flexible cylinder by such a limited discretization of the physical system is the most important shortcoming of the spring-mounted experiments when used to predict the response of flexible risers.

Griffin (1972) performed flow measurements in model tests with spring-mounted and oscillated circular cylinders. He observed that the vortex shedding patterns from both types of tests were found to be correlated in phase for 8-10 diameters along the cylinder length under resonant and synchronized conditions. Stable vibrations of the cylinder occur when the peak-to-peak amplitude of the self-excited motion approaches ten percent of a diameter, and this behavior was previously observed for both self-excited and forced vibrations [Koopmann (1967)]. He concluded that carefully executed oscillated cylinder model tests will produce equivalent results to tests of spring-mounted cylinders.

3.4.3 Flexible Cylinders

Flexible cylinders are those whose natural bending frequencies are within the range of expected vortex shedding frequencies. Therefore, flexible cylinders will vibrate in flexure due to vortex shedding effects when placed in a flow stream. The cylinder vibration will interact with the incoming flow, resulting in a complicated fluid-structure interaction system.

The advantage to flexible cylinder experiments is that they can incorporate additional effects associated with the three-dimensional nature of the flow. For example, in flexible cylinder experiments it is possible to model situations where excitation force is applied to a portion of the cylinder, with the rest of the cylinder contributing primarily hydrodynamic damping. Flexible cylinders have also been used to investigate broad-band strumming response often seen in sheared flow on cables [Vandiver et. al. (1988), (1987)]. Finally, since flexible cylinders respond in a variety of flexural modes, the effects of phase between displacements at different parts of the cylinder (e.g. portions of the cylinder vibrating in opposite directions) can be investigated.

For the most part, detailed force data is not available for flexible cylinders. Typically accelerations are measured at one or more points along the cylinder, from which displacement amplitudes and frequencies can be calculated. These data can be difficult to apply directly in engineering models of VIV, as they represent the result of a complicated hydrodynamic interaction and a complicated dynamic response of a flexible structure. However, these data are clearly useful for bridging the gap between detailed knowledge of applied force on stationary cylinders and the dynamic response of real structures. They are also potentially useful for verifying predictive models.

3.4.4 Oscillated Cylinders

Iwan and Blevins (1974) claimed that there is no fundamental fluid mechanical distinction between forced cylinder motion and elastically-mounted cylinder motion, if it is assumed that the force between the cylinder and the fluid depends only on the weighted average velocity and acceleration of the fluid relative to the cylinder. Stansby (1976), relative to lock-in model tests of circular cylinders in uniform and shear flow, argued that to investigate the relationship between the vortex shedding frequency, the cylinder's oscillation frequency, and the amplitude of oscillation, it is better to drive the cylinder mechanically. He suggested that this was necessary, because lock-in causes the vortex shedding to be almost perfectly correlated across the span, which in turn causes the amplitude of vibration to increase. Thus experiments in which a cylinder is spring-mounted and free to vibrate may be more difficult to interpret than oscillated cylinder experiments.

Botelho (1983) indicated, with reference to Hall (1981), that there might be some doubts about the analogy between the oscillated cylinder and the spring-mounted cylinder and the experimental use of one situation to understand the other. But Botelho concluded, at least qualitatively, that force measurements from oscillated cylinder experiments can be used to predict amplitudes and frequencies of spring-mounted cylinders.

Moe at al. (1989), and Wu (1989) also claimed that results from oscillated cylinder tests can be used to predict amplitudes of a spring-mounted cylinder. Overall, they concluded that oscillated cylinder tests agree reasonably well with spring-mounted cylinder tests when the "true" reduced velocity (Vr=V/f*D, where: D=cylinder diameter, V=flow velocity, and f=actual vibration frequency of cylinder - instead of the usually used natural frequency) is used in the comparisons, especially when the in-line direction is spring supported. However, some considerable deviations were apparent, especially for the spanwise correlation of the lift force.

For self-excited vibrations in the lock-in region, nearly harmonic oscillations will occur. The displacement spectra have narrow bandwidths, yet 10% variation in peak amplitudes is common and the associated force amplitudes are strongly irregular. Oscillated tests typically employ harmonic motions, and the associated force amplitudes vary much less from cycle to cycle. Therefore, the average lift force for the self-excited case cannot be assumed to equal the lift force for the forced-vibration case, even though the average motion amplitudes are equal [Moe et. al. (1989)].

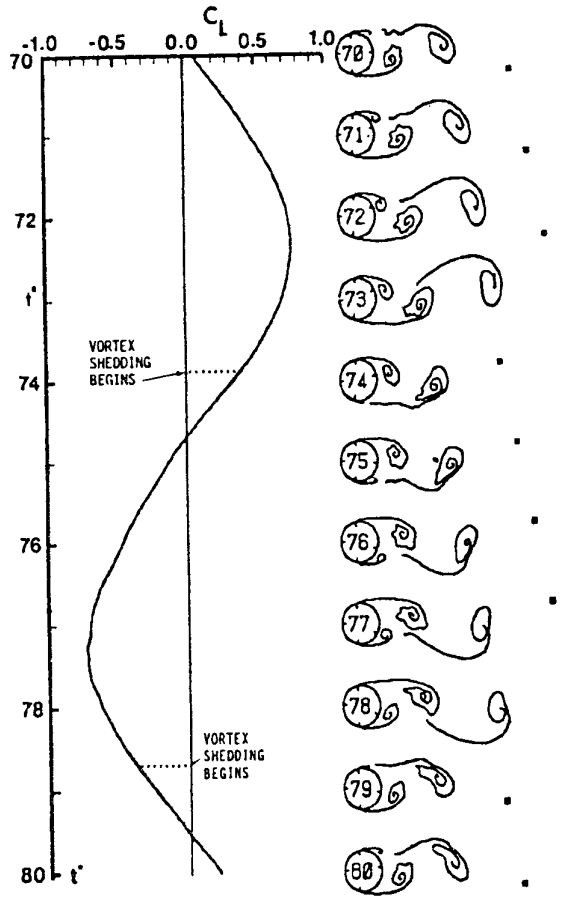

FIGURE 4.1 LIFT FORCE PICTURE ON STATIONARY CYLINDER (SARPKAYA 1979)

One factor is that a cylinder, undergoing nearly harmonic vibrations of gradually changing amplitudes experiences different forces at a given amplitude compared to the regular oscillations at the same amplitude (separation points and pressure distributions, and thus forces and motions, will be influenced by the previous patterns due to the so-called "history effects"). Also it must be remembered that the lift force components as a function of amplitude are not linear, and thus the average forces (derived from analysis of irregular time series of the lift force in self-excited tests) will differ from the forces at the average amplitude (from the analysis of the regular time series in forced-vibration tests). Therefore, the assumption that force coefficients from oscillated cylinder tests can be used to predict self-excited motions must be verified experimentally. Some verification along these lines has been done [Sarpkaya (1977)].

4.0 LIFT FORCE

The dynamic force in the direction transverse to the flow direction due to shedding vortices from alternate sides of the cylinder is conventionally referred to as lift force. This force arises as a direct result of the fluctuating pressure distribution that occurs on a bluff body during the vortex shedding process. Figure 4.1 illustrates one cycle of lift force on a stationary cylinder in steady flow at a subcritical Reynolds number. Lift force is often characterized by its magnitude, frequency content and some measure of correlation between forces applied at different locations along the cylinder.

4.1 Lift Force Magnitude

Lift force coefficient is the most commonly reported parameter in the test literature. Lift coefficient is most often referred to as C_L, and is typically defined for a cylinder as:

$$C_L \equiv \frac{F_L}{\frac{1}{2}\rho DLV^2}$$

where F_L is the measured lift force, ρ is the fluid mass density, D is the cylinder diameter, L is the cylinder length, and V is the flow velocity. In model tests on stationary cylinders, the lift force is measured directly by force transducers (force elements) or is derived from measurements using strain gauges or pressure transducers.

Force transducers usually measure total force on a test section of the cylinder. In uniform flow, force amplitude is constant along the test section. However, it is essential to recognize that the dynamic lift force may not be well-correlated along the test section. Therefore, when using force transducers and seeking the local lift force amplitude it is necessary to correct for the spanwise correlation of vortex-induced forces. Many authors report values of lift coefficient without any adjustment. Due to this, lower lift coefficient values will be reported when forces are less correlated along the length of the test section.

Correlation length seems to depend on many different factors, one of the more important being oscillation amplitude. Forces on stationary cylinders can be correlated over lengths of one to six diameters, while forces on oscillating cylinders can be correlated for up to 100 diameters. Essentially, all nominal lift coefficient values (i.e. unadjusted for correlation effects) obtained from model testing implicitly reflect the degree of spanwise force correlation present during the test. If these coefficients are then used in a predictive model, the results are only appropriate for forces with correlation characteristics similar to forces experienced during the model test. An alternative is to correct for correlation effects in the determination of lift coefficient (i.e. use a lift coefficient corresponding to perfectly correlated force) and include a correlation factor in the predictive model. Correlation length is discussed in detail in Section 4.3.

Pressure transducers generally produce more accurate results for the lift force because they measured the pressure distribution of the fluid around the cylinder's circumference. Thus, they are less likely to be adversely affected by lack of spanwise correlation of the force. However, their installation and calibration is cumbersome and tedious.

The definition of lift force is more complex, and interpretation of lift data becomes more difficult, when the body moves relative to the flow. Figure 4.2 illustrates the wake of an oscillating cylinder in a uniform flow at different oscillation amplitudes. Note how the wake direction is affected by cylinder motion. The changing direction of the wake causes drag and lift forces to rotate relative to the cylinder axis. Like the stationary cylinder case, there is no question that a cylinder oscillating transversely to the flow experiences hydrodynamic forces due to the shedding of vortices. However, the applied hydrodynamic force now contains components due to the cylinder's motion relative to the fluid, and there is no rigorous way to separate them.

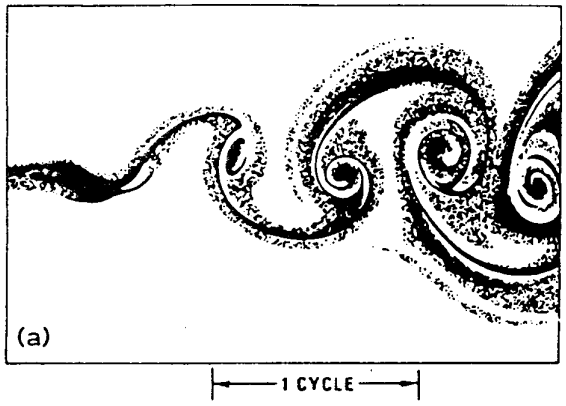

(a) Stable staggered vortex street; $A_y/D = 0.5$.
(b) Unstable pattern with three vortices formed per cycle of vibration; $A_y/D = 1.0$ (Griffin and Ramberg, 1974).

FIGURE 4.2 WAKE OF OSCILLATING CYLINDER AT RESONANCE (BLEVINS 1990)

Conceptually, lift is a transverse component of force occurring at the vortex shedding frequency. Lift will be influenced by body motion, and there is considerable evidence demonstrating the influence of body motion on lift force frequency and correlation. But it is an applied force which owes its existence to the character and strength of the hydrodynamic wake formed by flow around the body, not the motion of the body itself. On the other hand, damping and added mass are terms defined by motion of the body in a fluid, although the wake undoubtedly has some influence on these forces as well. Damping is often assumed to be the transverse force component 180° out of phase with cylinder velocity, with added mass the term proportional to and 180° out of phase with cylinder acceleration. However, to date no simple model with lift, added mass, and damping terms has been shown to adequately describe the transverse force experienced by an oscillating cylinder in steady flow.

TABLE 4.1 COMPILATION OF LIFT COEFFICIENT FROM STATIONARY CYLINDER DATA

Curve #	Authors	Low Re	High Re	Medium	Value	Comments
1	Bingham et al. (1952)	8.0E+04	8.0E+04	air	mean peak	shock tube, uniform flow, few oscillation cycles of lift force
2	Bishop - Hassan (1963)	4.0E+03	1.2E+04	water	mean peak	rigid cylinder, strain gage measurements
3	Bublitz (1971)	9.0E+04	7.5E+05	air	rms	
4	Chen, Y. N.	4.0E+01	5.0E+05	air	peak	smooth cylinder, uniform flow, low turbulence (calculation)
5	Chen, Y. N.	4.0E+01	5.0E+05	air	peak	rough cylinder, uniform flow, high turbulence (calculation)
6	Chen (1969)	6.0E+03	6.0E+03	air	rms	
9	Dawson - Marcus (1970)	9.0E+01	9.0E+01	air	mean peak	
10	DnV	1.0E+04	8.0E+06	air/water	rms	uniform flow
11	Fung	1.0E+05	6.0E+05	air	rms	uniform flow, strain gauges, L/D=6 (overall), L/D=2 (instrum. section)
12	Fung (1960)	1.8E+05	1.4E+06	air	rms	uniform flow, strain gage measurements, L/D=6, L/D=2 (instrum. section)
14	Goldman (1957)	1.8E+05	2.5E+05	air	peak	bottom curve of Goldman curves
15	Goldman (1957)	1.8E+05	2.5E+05	air	peak	top curve of Goldman curves
16	Humphreys	4.5E+04	2.0E+05	air	rms	force measurements with load cells, L/D = 6.5, uniform flow
17	Humphreys	4.0E+04	6.0E+05	air	peak	force measurements with load cells, L/D = 6.5, uniform flow
18	Humphreys (1960)	2.0E+03	1.2E+06	air	mean peak	force measurements with load cells, L/D = 6.5, uniform flow
19	Huthloff	3.0E+04	1.0E+05	air	rms	uniform flow, strain gauge and inductive transducer measurements
20	Jones	4.0E+05	2.0E+07	air	rms	force transducers, L/D=5.33
21	Jones (1968)	2.0E+06	2.0E+07	air	rms	force transducers, L/D=5.33
22	Jordan - Fromm (1972)	5.0E+02	5.0E+02	air	rms	uniform flow (calculations)
23	Keefe (1962)	1.0E+04	1.0E+05	air	rms	direct force transducer
24	King	4.0E+04	4.0E+04	water	rms	uniform flow
25	Macovsky (1958)	2.0E+04	8.0E+04	water	peak	force measurements
26	Macovsky (1958)	3.7E+04	1.1E+05	water	mean peak	force measurements
27	McGregor (1957)	4.0E+04	1.8E+05	air	rms/mean peak	top curve (mean peak), uniform flow, pressure measurements/integration
28	Moeller - Leehey	1.9E+04	1.9E+04	water	rms	force measurements, rigid cylinder, L/D = 28
29	Phillips (1956)	3.0E+01	2.0E+02	air	mean peak	uniform flow, questionable data points (from Y. N. Chen paper)
30	Protos et al. (1968)	4.5E+04	4.5E+04	water	rms	uniform flow, cantilever piercing free surface, L/D = 6.5
31	Rajaona - Sulmont	3.0E+04	1.8E+05	water	peak	towed, fixed cylinder, force measurements, L/D=2.5
32	Rajaona - Sulmont	3.0E+04	1.8E+05	water	rms	towed, fixed cylinder, force measurements, L/D=2.5
33	Rodenbusch et. al. (Shell)	2.0E+05	2.2E+06	water	peak	steady tow, smooth flow, strain gages, L/D=2.8, 1 (instrumented section)
34	Ruedy	1.0E+05	1.0E+05	air	rms	rigid cylinder, uniform flow
35	Sallet	1.0E+02	1.0E+06	air	peak	theory, based on wind stationary pressure tap measurements
36	Schewe (1983)	1.0E+04	8.0E+06	air	rms	force measurements, clamped ends, L/D=10
37	Schmidt et al. (1966)	1.0E+05	1.0E+07	air	rms	CLo related to infinitely thin strip, pressure measurements/integration
38	Schmidt (1965-66)	3.0E+05	7.0E+06	air	rms	uniform flow
39	Schwabe (1935)	7.0E+02	7.0E+02	water	mean peak	uniform flow with turbulence, pressure measurements, (calculations)
40	Sonneville	1.0E+04	3.0E+04	water	mean peak	uniform flow
41	Surry	5.0E+04	5.0E+04	air	rms	rigid cylinder, turbulent flow
42	Vickery - Watkins (1962)	4.0E+04	1.8E+05	air/water	rms	stationary and oscillating cylinder data
43	Vickery - Watkins	1.0E+04	1.0E+04	air	rms	rigid cylinder, pivoted ends
45	Weaver (1961)	7.0E+04	3.0E+05	air	peak	rigid cylinder, Iu=0.5%, uniform flow, force measurements, L/D=10-15
46	Whitney et al.	1.0E+02	2.0E+07	air	rms	based on air stationary experiments, uniform flow (calculations)
47	Woodruff - Kozak	2.0E+05	2.0E+05	air	rms	uniform flow

In the following sections, lift coefficient data from primarily stationary cylinder tests reported in the literature are compiled and presented versus Reynolds number. Lift coefficient values are then reported separately for stationary cylinders in air and water. Data on fluid-structure interaction (including variation in apparent lift with response amplitude) are presented in subsequent sections. The objective of this material is to present the reader with the information required to quickly find and effectively utilize lift coefficient data that exists in the public literature. However, when utilizing these data in a predictive model, the reader is urged to consult the original publication to acquire a thorough understanding of the assumptions and limitations inherent to each particular data set.

4.1.1 Reynolds Number Dependence

A large number of model tests have been published that attempt to address the variation in lift force with Reynolds number. A compilation of published lift coefficient data is presented in Figure 4.3. These data were collected from individual studies and from other data reviews (e.g. Sarpkaya et. al. (1981), Chen (1972)). A few lift coefficient values reported in the literature were derived from drag coefficient model tests using the momentum balance method [Chen (1972), Sallet (1975, 1973)]. Related information about each model test is summarized in Table 4.1.

The compiled data in Figure 4.3 relate to model tests in uniform flow for stationary cylinders at various aspect ratios. Surface roughness and turbulent intensity of the approaching flow were generally small. Lift coefficients are reported as rms, mean amplitude, or peak values. The tests were usually performed at a single Reynolds number or over a small range of Reynolds numbers. Test facilities include wind tunnels, water channels, and U-tubes. Modeling of flow conditions was accomplished using fan-generated wind, pump-generated wind, pump-generated water current, and tow carriages in calm water.

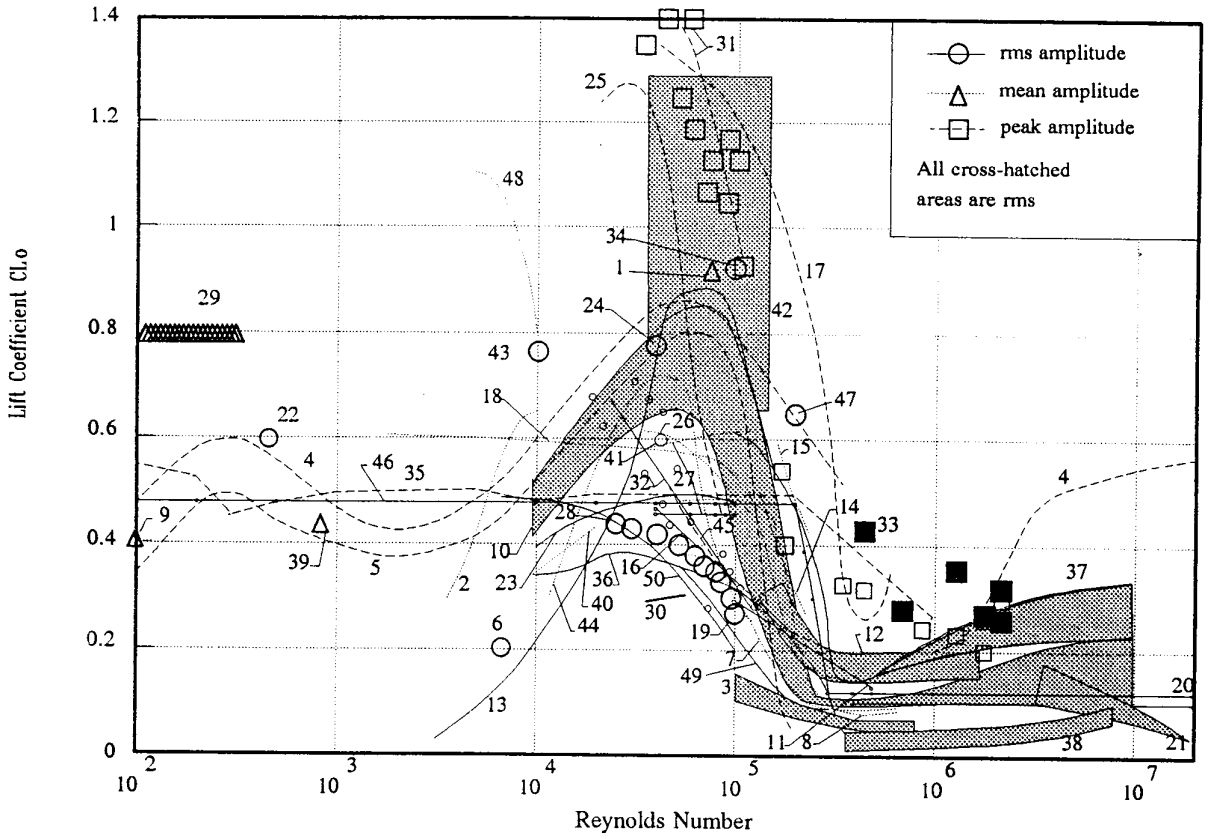

FIGURE 4.3 LIFT COEFFICIENT DATA FOR STATIONARY CYLINDERS

An example of lift coefficient behavior in subcritical up to postcritical flow is that of Schewe (1983) for a stationary cylinder in wind flow. Lift coefficients were measured by force transducers. Time series of the lift fluctuations are shown in Figure 4.4. This lift coefficient behavior is typical for the individual Reynolds number ranges. All amplitudes are normalized to their corresponding rms values and the dotted lines are equivalent to ±3*rms. The time axis was scaled with the inverse Strouhal number, $1/S_t=T*U/D$ (where S_t=Strouhal number, U=current velocity, D=cylinder diameter, and T=characteristic period); so that all time functions are directly comparable with respect to their characteristic time T. The time series in Figure 4.4c taken at $Re=2.6x10^6$ (supercritical) is dominated by random fluctuations of the lift. This visual impression is confirmed by the corresponding probability density which is nearly Gaussian. The time series of lift coefficient in the subcritical, transitional, and postcritical ranges look like sine waves which are randomly modulated in amplitude and frequency.

Schewe reported his lift coefficients without adjusting for spanwise correlation of the lift force. Schewe observed variations in spanwise correlation which led to peak lift coefficients up to +3*rms in the subcritical state, and about +4*rms in the super- and postcritical states. He also observed that the apparent modulation frequency of the lift was strongly correlated with the drag. This means that if the amplitudes of the lift fluctuations are increasing, i.e. the coherence along the span of the cylinder increases, then the drag also increases and vice versa.

Independent of model test conditions (fluid medium, value reported and test cylinder category) the lift coefficient follows similar qualitative characteristics, as seen in Figure 4.3. First, C_L does not vary substantially with increase in Reynolds number up to 10^4. Most of the test data [points 9, 22, 39, and sections of curves 4, 5, 35, 46] reside between a lift coefficient of 0.4 and 0.6 independent of the value classification (rms, mean amplitude or peak), the test medium or the test cylinder condition.

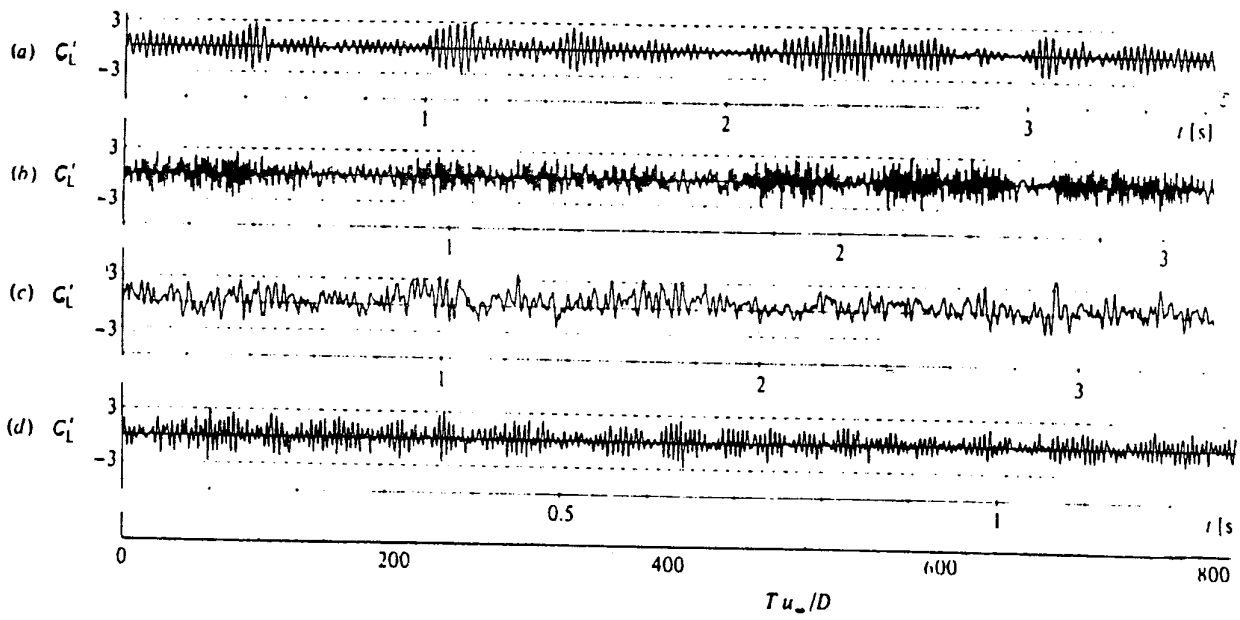

a) Subcritical Flow: Re = 5.1×10^4
b) Supercritical Flow: Re = 3.5×10^5
c) Supercritical Flow (Upper Transition): Re = 2.6×10^6
d) Transcritical Flow: Re = 7.1×10^6

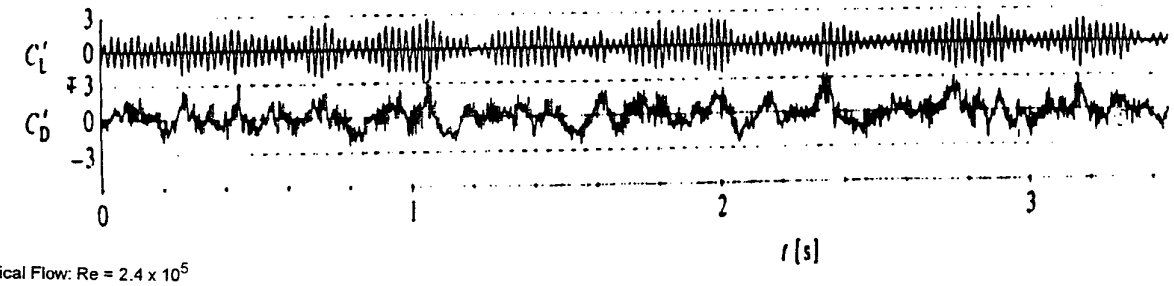

Subcritical Flow: Re = 2.4×10^5
C_L and C_D amplitudes are normalized with the corresponding r.m.s. values

FIGURE 4.4 TIME SERIES OF LIFT AND DRAG (SCHEWE 1983)

At the end of the subcritical range the lift coefficient starts rising. It attains a maximum value near Reynolds numbers around $8x10^4$, and then decreases throughout the transition range. Scatter of the data reported within this range is substantial. Maximum rms coefficient varies from 0.4 [curve 19] to 1.3 [cross-hatched area 42]. Note that data in curve 42 includes stationary and oscillating cylinder data. Oscillating cylinder data tend to yield different "lift" coefficients for a variety of reasons as discussed previously. It is also the case that correlation lengths seem to increase substantially in this range (see Section 4.3), and therefore substantial differences in nominal lift coefficients are to be expected. Maximum mean amplitudes in this range vary from 0.6 [curve 18] to 0.9 [point 1]. Maximum peak lift coefficients range from 0.8 [curve 5] to 1.4 [curve 31].

At Reynolds numbers in the critical regime, reported lift coefficient values drop abruptly. The organized shedding disappears in the critical flow regime, thus the fluctuating lift drops to a lower value and becomes relatively constant up to the supercritical flow regime. The drop in the lift coefficient value has been captured in most of the compiled test results. The exact Reynolds number range, however, where the drop occurs shows some discrepancy, similar to that of the occurrence of the maximum lift coefficient value. It appears that the drop of the lift coefficient occurs for Reynolds number between 10^5 - $3x10^5$. The lift coefficient value varies between 0.05 - 0.3. The rms lift coefficient shows an average value of 0.2, the mean amplitude of 0.1, and the maximum peak of 0.35. The maximum peak value appears consistent with the rms value, but the data on mean amplitudes appears low.

The character of the wake changes rapidly and substantially around $3x10^5$ for smooth cylinders in steady flow. This change in flow character includes the transition of the boundary layer from laminar to turbulent, a narrowing and disorganization of the wake, and accompanying drops in drag and lift forces. It is also well known that the onset of this transition can occur at smaller Reynolds numbers due to a variety of causes such as small increases in surface roughness, or turbulence in the incident flow. Some of the lower maximum lift coefficient values reported could be affected by an early transition of this type during the tests.

After the transition, C_L remains approximately constant. Most of the data in this regime have been produced from model tests in wind tunnels due to a lack of test facilities able to achieve these flow conditions in water. The exceptions are tests performed by Shell Development Company [points 33, Rodenbusch et. al. (1983)]. Overall, the limited data in this regime indicate nearly constant values for the lift coefficient.

4.1.2 Data Scatter

The upper subcritical Reynolds number region between 10^4 and $1.5x10^5$ exhibits the most scatter in lift coefficient values. Surprisingly, scatter is more pronounced in the rms values of the lift coefficient than in the mean amplitude and maximum peak values.

Scatter in rms values for Reynolds numbers between 10^4 and $1.5x10^5$ bears further scrutiny. The rms data fall into two distinct groups. The first group [curves 16, 23, 27, 36; points 19, 28, 32] includes maximum rms values around 0.4 - 0.5. The value of point 30 is only 0.3, but the test used a cantilever cylinder with an aspect ratio of 6.5, which may have contaminated the lift force measurement (3-D effects with vortices wrapping vertically around the free end). The value of point 28 is 0.43, and is somewhat typical for experiments using a stationary cylinder in a water channel.

The second group [curve 13; cross-hatched curves 10, 42; points 24, 34, 41, 43, 47] shows maximum rms values varying between 0.6 - 1.3. The cross-hatched area 42 [Vickery et. al. (1962)] is very interesting because it suggests high variation of the lift coefficient in a small range of Reynolds numbers. These data represent several different tests, including wind tunnel and water channel apparatus, cantilever and pivoted rigid test sections, and using both stationary and oscillating cylinders.

Scatter can be attributed to various causes. Humphreys (1960) has experimentally demonstrated the effect of the end gaps. He obtained larger lift coefficients when cylinder ends were sealed at the wall. Many researchers note the sensitivity of lift force to stream turbulence [Surry (1969), Batham (1973), Cheung et. al. (1983), etc]. The degree of rigidity of the mounting of the cylinders may also play an important role [King (1977)] as cylinder oscillations at the end boundaries can contaminate the vortex shedding. Three-dimensional effects where the vortices wrapped vertically along the cylinder length [Vickery (1962) Protos (1968) etc.] also affect the vortex shedding process and the pressure field around the test cylinder.

The test cylinder aspect ratio can also affect the measured lift forces and contribute to the scatter of lift force measurements from different model tests. As discussed previously, if the cylinder is long compared with the correlation length, spatial correlation of lift along the cylinder is reduced, causing reduction of the net lift force. Keefe (1962) was able to vary the oscillatory forces on a cylinder by attaching concentric discs perpendicular to it. A decrease in disc spacing form 18D to 3D (D is cylinder diameter) increased the oscillatory forces by 35% and it must be concluded that the discs split the cylinder into a series of well correlated, contiguous sections. Several other researchers have studied the correlation of the lift forces and reached similar conclusions [Toebes (1969), Ramberg et. al. (1976)].

Wide variation of forces can be measured on apparently identical cylinders in different test facilities. The blockage ratio (ratio of cylinder diameter to width of test facility) may effect the flow characteristics and thus the lift coefficient [Modi et. al. (1975), Cheung et. al. (1980)]. Additionally, the force measuring method may influence the recorded values as discussed in previous paragraphs.

As discussed in Section 4.1.1, despite significant scatter all the data are qualitatively consistent across a broad range of Reynolds numbers. In general, much of the quantitative difference in rms, mean amplitude, or peak lift coefficient at any given Reynolds number can be attributed to differences in testing technique (e.g. stationary vs. oscillated cylinders) as well as in test medium (water vs. air). These differences lead to variations in behavior of the shedding process, which result in reports of substantially different values for lift coefficient. The key to extracting useful information from the compiled data is to first understand the essential differences affecting each data point and then intercept the data in a manner consistent with the proposed analysis model.

In wind tunnel tests, wind turbulence and tunnel wall anomalies have historically affected the results, producing lower force values. Turbulence reduces correlation of the vortices along the cylinder axis, resulting in lower measured lift and lower lift coefficients. On the other hand, oscillating cylinders in water experience substantial forces due to cylinder motion that are not always accounted for in lift force measurements, leading to higher or lower reported values of the lift coefficient. Furthermore, forces on stationary cylinders (in air or water) tend to be less correlated than forces on oscillating cylinders (see Section 4.3), leading to low nominal lift coefficient values.

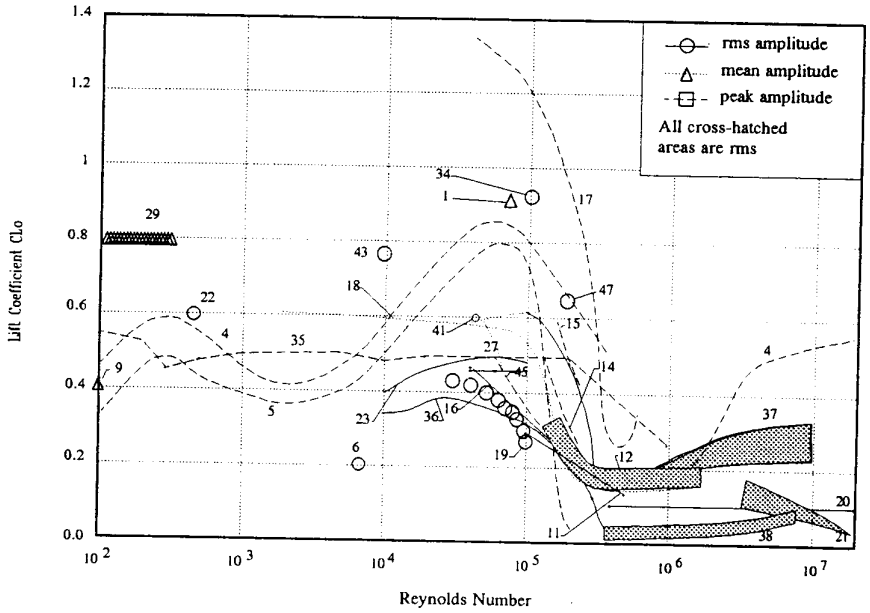

FIGURE 4.5 LIFT COEFFICIENT FOR STATIONARY CYLINDERS (IN AIR)

To more readily illustrate such differences, data from stationary tests are discussed and presented separately by testing technique and test medium in the following sections.

4.1.3 Stationary Cylinders in Air

All data on stationary cylinders tested in air are compiled in Figure 4.5. The majority of the test data were derived from force measurements (force transducers, force cells, and strain gauges). Only curves 11, 12, 27, 35, and 37 were derived from pressure measurements.

Lift force measurements in wind tunnel tests can be affected by:

- non-uniformity of flow across the wind tunnel (probable decrease in measured lift force due to "shear flow" equivalent effects - reduction of correlation length and shifting of Strouhal frequency),
- blockage (probable increase in measured lift force)
- turbulence (decrease in measured lift force in subcritical flow regime, slight increase in supercritical flow regime),
- low aspect ratio cylinders (increase in measured lift force per unit length),
- effects of interaction and 3-D effects from end-support mechanisms (probable decrease in lift force due to breaking of 2-D vortex shedding process).

The following comments refer to the data in Figure 4.5.

Curves 4, 5, (Chen, 1972), and 35 (Sallet, 1973, 1975) represent theoretical estimates of peak lift coefficient based on experimental results of the drag coefficient and the theorem of momentum conservation. Curve 4 refers to a smooth cylinder in non-turbulent flow, while the curve 5 was derived for a more typical cylinder with small roughness in a turbulent flow. The lift coefficient estimate is less for the turbulent flow than that in smooth flow due to the breaking up of the lift force correlation along the cylinder length [Cheung et. al. (1983)]. Chen did not derive correlation length values in his study. Instead the lift coefficient was derived by using among other parameters the longitudinal and lateral distance of successive vortices which have an implicit relation to correlation length. Chen compiled correlation length data from other authors and argued that the high values of lift coefficient coincide with high correlation length values for Reynolds numbers 10^4-10^5. The maximum lift is 0.8, which disagrees with the 1.4 value from model tests. However, Chaplin (1972) pointed out that Chen had omitted in his calculations a circulation term that could give a higher lift coefficient up to 1.8, which is higher than comparable experimental results.

The maximum lift coefficients in curve 35 appear low compared to Chen's curves for Reynolds number 10^4-10^5.

In addition, the lift variation in the subcritical regime from curve 35 is different than the majority of the test data.

Humphreys (1960) performed tests with stationary cylinders of aspect ratio L/D (L=Length, D=Diameter) of 6.5 in a wind tunnel, measuring lift force by force transducers (load cells). Curves 16, 18, and 17 represent rms, mean amplitude and peak lift coefficients, respectively. Humphreys' curve 18 of mean amplitude lift coefficients agrees well with McGregor's mean amplitude lift coefficient curve 27 which was derived by pressure measurements. Since correlation length is about 6 diameters for stationary cylinders at Reynolds numbers 10^4-10^5 (see Section 4.3), the force is probably fully correlated along the cylinder length. Consequently, lift force per unit length obtained from dividing total force by cylinder length will be reasonably accurate, and will agree with lift coefficients derived from integration of pressure measurements.

Curves 16, 23, 27, 36, and 19 represent rms lift coefficient values derived by force measurements for Reynolds numbers 10^4 - 10^5. The test cylinder aspect ratios were 6.5 and 10 for curves 16 and curve 36, respectively (data could not be located for the other curves). Rms lift coefficients from all curves follow similar patterns. However, the low aspect ratio test produced 20% higher lift coefficients than the highest aspect ratio at Reynolds number $5x10^5$. This is expected because the lift force is not fully correlated for the cylinder with the highest aspect ratio.

Peak lift coefficients derived from model tests are presented in curves 14, 15, 17, and 45. Peak lift is about 1.3 at Reynolds number of $5x10^4$ (Humphreys' data from fully correlated cylinder tests). The lift coefficients of all 4 curves appear qualitatively consistent in the critical regime, where they drop sharply to 0.3 at Reynolds numbers of $1.5\text{-}2.5x10^5$. The variation in Reynolds number at the drop in lift may be due to slight variations in turbulent intensity and cylinder surface roughness among model tests. These small flow and cylinder geometry variations cause the characteristic boundary layer, wake, and pressure distribution changes to occur at slightly different Reynolds numbers.

Correlation effects are very important in the critical flow regime, where the correlation length becomes very small. At critical Reynolds numbers, measured lift forces are relatively low, in part due to lack of force correlation. This lack of force correlation is often reflected in the lift coefficients themselves, as most researchers have not corrected their data for correlation effects.

The limited data in the supercritical flow regime indicate nearly constant values for the lift coefficient at an average value of 0.15 (curves 11, 12, 20, 21, and 38). Curves 11 and 12 from Fung (1960) yield an average rms lift coefficient of 0.2. Similarly, curves 20 and 21 from Jones et. al. (1969) with a cylinder aspect ratio of 5.25, appear consistent and repeatable with an average rms lift coefficient of 0.1. Jones measured transverse force by force transducers.

However, test results by Schmidt [curve 37], from Wootton et. al. (1971), indicate increasing lift coefficient values for Reynolds numbers about 10^7. Results were based on the lift force for an infinitely thin strip (pure 2-D flow conditions) in a wind tunnel. The lift coefficient was derived from pressure measurements and pressure integration. Wootton et. al. (1971), suggested that pure 2-D flow conditions are not necessarily valid in the wind tunnel because of end effects and interaction with incoming flow.

Two reasons were given for the differences between data in curve 37 and curve 38, both measured by Schmidt: turbulence in the flow conditions and/or an increase of the vortex correlation length for curve 37. The existence of turbulence at very high Reynolds number could reduce the velocity into the free shear layers and cause the wake to fluctuate more, effectively broadening the wake. The swinging of the wake, in effect, induces a slight increase in the fluctuating lift [Cheung et. al. (1983)]. An increase in correlation length in the postcritical Reynolds number range would also produce higher lift forces. However, Chen (1972) observed that the vortex correlation length in the postcritical Reynolds number range has the same order of magnitude as in the critical Reynolds number range, where it is small.

In summary, the rms lift coefficient in air is about 0.4 for Reynolds number < 10^4, increases to its maximum rms value of 0.6 at Reynolds number about $8x10^4$, (maximum peak value of 1.3) then decreases to 0.2 (Re about $3x10^5$) and remains approximately constant for higher Reynolds numbers. The data indicate a small increase to 0.3 for postcritical flow.

4.1.4 Stationary Cylinders in Water

Lift coefficient data from tests on stationary cylinders in water are compiled in Figure 4.6. In a water tank, measured lift force data can be affected by:

- carriage vibration (probable increase in measured lift force, especially if carriage vibrates within the range of forcing frequencies),
- blockage ratio (as in wind tunnel tests only when cylinder is fixed and water is flowing; when cylinder is towed, blockage will not have any effect)
- non-uniformity of flow across the water tank (as in wind tunnel tests),
- generation of turbulence (usually does not have as strong effect as in wind tunnel tests)

- low aspect ratio cylinders (as in wind tunnel tests),
- effects of interaction and 3-D effects from end-support mechanisms (usually does not have as strong effect as in wind tunnel tests, especially when end-plates are used).

The stationary cylinder data by Bishop et. al. (1964), [curve 2] obtained from Sarpkaya et. al. (1981), showed a high jump of the lift coefficient, from 0.3 to 0.63, in a relatively small Reynolds number range, $4x10^3$-$1.1x10^4$. Their data represent mean amplitude values obtained from stationary cylinders in flowing water in a water flume, and they are the most widely quoted data in the literature. They measured lift force by force transducers. In Sarpkaya's discussion there is no mention of correlation effects on the measurements. Note that the jump occurs at the same Reynolds numbers as a substantial increase in correlation length (see Section 4.3).

Point 28, Moeller et. al. (1982), was derived from experiments with an aspect ratio of 28 and end-plates. They measured transverse force by force transducers. The cylinder was mounted on a towing carriage, moving with uniform speed. Moeller's tests were very carefully planned and executed at MIT's water tank. The rms lift coefficient and shedding frequency were determined from the spectrum of the lift force signal at the Reynolds number $1.93x10^4$. The peak in the lift force spectrum was at the vortex shedding frequency. The rms lift coefficient was 0.43 at Strouhal number 0.19. The high aspect ratio indicates that forces were probably not fully correlated along the cylinder length. The lift coefficient is lower than Rajaona's (curve 32) where the lift force was probably fully correlated along the cylinder length (aspect ratio 2.5, discussed below).

Curve 30, Protos (1968) was derived from stationary tests using a cantilever cylinder with aspect ratio of 6.5, piercing through the free surface of the water tank. A small gap existed between the cylinder cross section and the tank bottom. Lift force was measured by force transducers and rms lift coefficients were derived by spectral analysis. Rms lift coefficient values are low for the test Reynolds numbers of 4.0-$4.6x10^4$. A possible explanation for the low lift values is that three-dimensional wrapping of the vortices shed at the free surface may have disrupted the force correlation along the cylinder.

The maximum lift coefficient is 1.4, which was measured in model tests by Rajaona et. al. (1988) [curve 31, and points 31]. Rajaona's tests used a fixed cylinder towed with constant speed (uniform flow conditions) in a water channel. The lift coefficient was derived from force measurements (load cells), and the aspect ratio was 2.5. From data in Section 4.3, correlation length varies substantially (6 diameters to 1 diameter) within this Reynolds number range. Rajaona derived peak and rms lift coefficient values, curves 31 and 32, respectively. Estimates show that peak values are about 2.1 times the rms values.

Curve 25 from Macovsky (1958), presents lift coefficient peak values close to Rajaona's data. The maximum 1.26 value is slightly shifted to a lower Reynolds number, but a small difference in cylinder roughness between the two tests could count for this. Macovsky derived peak and mean amplitude lift coefficients, curves 25 and 26, respectively, from force measurements. In addition, Rajaona's rms lift coefficients (curve 32) and Macovsky's mean amplitude coefficients (curve 26) show similar variation with Reynolds number. Their data also indicate good quantitative agreement, with the mean amplitude values slightly higher that the rms lift coefficient values.

Test points 33 represent Shell's data [Rodenbusch et. al. (1983)]. Shell's tests used smooth cylinders under steady speed tow, and strain gages to measure forces. The length of the instrumented cylinder was 1D (D=diameter), and the overall length was 2.8D (0.9D long dummy cylinders were placed at each side of the instrumented cylinder). The overall cylinder aspect ratio was 2.8D, which could have led to fully correlated lift forces along the cylinder length, (correlation length is about 1-3D for the test Reynolds numbers). However, it could have also resulted in two overlapping end cells (see Section 4.2.3). The peak lift coefficient decreases almost linearly from 0.6 at Reynolds number $2x10^5$ to 0.2 at Reynolds number $2x10^6$.

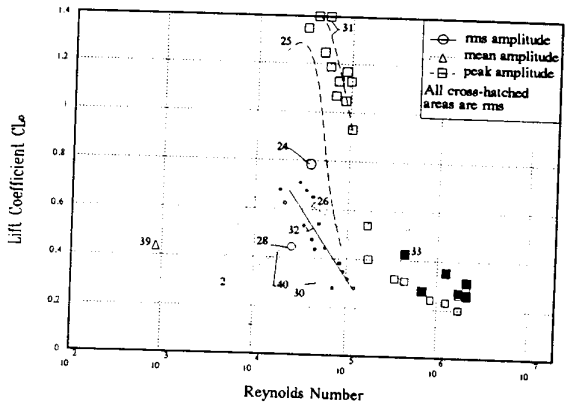

FIGURE 4.6 LIFT COEFFICIENT FOR STATIONARY CYLINDERS (IN WATER)

The filled-in squares represent carriage towing in the positive X direction and the empty squares carriage towing in the negative X direction. Shell reported that there was a large mean transverse force (about 10% of the drag force) when towing in the +X direction which was not present when towing in the -X direction. This phenomenon disappeared when roughness elements were attached to the cylinder. Shell concluded that some slight asymmetry of the cylinder or the top plate caused separation of the boundary layer when towed in the +X direction only.

However, it is well documented that for Reynolds numbers $2x10^5$-$8x10^5$ (critical to lower supercritical flow regime) there is a high mean lift coefficient [Schewe (1983), Bearman (1969)]. The boundary layer becomes turbulent at one side while it is still laminar at the other side of the cylinder. This produces an asymmetry in the pressure distribution around the cylinder, which subsequently produces a mean lift force. This force can be positive or negative, and is always oriented towards the cylinder side where the turbulent boundary layer forms.

Overall, lift coefficients reported for stationary cylinder tests performed in water are similar to those from tests in air as described previously. The rms lift coefficient from force measurements in water is about 0.4 for Reynolds number < $5x10^3$. Then, it increases to its maximum rms value of 0.6-0.7 at Reynolds number about $4x10^4$, where it remains constant up to Reynolds number 10^5. Then, it decreases to 0.3 (Reynolds number about $3x10^5$), and remains approximately constant at higher Reynolds numbers.

4.2 Lift Force Frequency

Lift on a cylinder in steady flow is an alternating force that in some cases is rather periodic in nature, while in other situations the force appears to be quite complex and random. A great deal of the available data comes from experiments on stationary cylinders, and consequently much has been established regarding the nature and characteristics of the lift force on stationary cylinders as characterized by the frequency content of either the force itself or flow velocities in the wake.

Lift force frequency is widely characterized by the Strouhal number, a nondimensional parameter of the form

$$S = \frac{fD}{V}$$

where f is a frequency associated with vortex-shedding, D is cylinder diameter, and V is the incident flow velocity. Note that the Strouhal number characterizes either a mean or a central spectral frequency, f, but gives no information regarding the range of frequencies present.

The shedding process ranges from regular, harmonic shedding, in which case f represents the simple harmonic frequency, to random, broad band shedding. In the broad band case f typically represents a mean spectral frequency. In all cases, f is often referred to as the Strouhal frequency, and is typically presented versus Reynolds number.

4.2.1 Reynolds Number Dependence

Experimental values for the Strouhal number measured on stationary cylinders in two-dimensional flow spanning the Reynolds number range $50<Re<2x10^7$ and a variety of surface roughness conditions have been compiled and are presented in Figure 4.7. Related information about each test is presented in Table 4.2. The majority of model tests were performed in a wind tunnel for a stationary cylinder, although a few tests have been performed with oscillating cylinders in water. Most of the Strouhal number data were derived from measurements of the velocity fluctuations in the wake, while fewer data were derived from the lift force spectra. Note, however, that lift force spectra are a more direct measure of the force characteristics than wake velocity measurements.

The behavior of the Strouhal number is stable for a wide range of Reynolds numbers, except around 10^6 (transitional region) where significant scatter occurs in the test data. There is little scatter in the data for Reynolds number up to 10^5 [curves 6, 15 20, 24, 26, 27, 29]. Vortices are shed very regularly in this region, resulting in an almost constant Strouhal number equal to 0.2.

In the transitional region, the Strouhal number becomes scattered varying from 0.05 - 0.5. Rapid increase of the Strouhal number at critical flow conditions has been observed by several authors. Delany & Sorensen (1953) found a sudden increase of their values of Strouhal number to 0.45 and then a decrease to 0.3 at about the same Reynolds number of $2x10^6$. This indicates the transition to postcritical flow conditions. Bearman (1969) measured a similar value of S = 0.46.

Also in the transitional range Achenbach and Heinecke (1981) found that smooth stationary cylinders had a chaotic, disorganized, high-frequency wake and Strouhal numbers as high as 0.5. Cylinders with some roughness (surface roughness $e/D=3x10^{-3}$ or greater, where e is the characteristic surface roughness) had organized, periodic wakes with Strouhal numbers S=0.25.

The scattering in the transitional region is associated with "weak" vortex shedding. Because of the irregular, random, and weak vortex shedding in the transitional region it is very difficult to collect and interpret model test measurements. Commonly, the Strouhal frequencies documented in the transitional region represent average values from multiple tests. Coder et. al. (1982) suggested that in the transitional Reynolds number regime, vortex-induced vibrations of cylinders generally occur at S=0.2 rather than the higher Strouhal numbers.

Vortex shedding from a stationary cylinder in the postcritical region does not occur at a single distinct frequency, but rather wanders over a narrow band of frequencies and it is not constant along the span [Blevins (1986); Schewe (1983); Jones et. al. (1969)]. However, the data scatter is not as extensive as in the transitional region. An average Strouhal number value is about 0.25 [curve 8, 11, points 22]. The curves obtained by Roshko (1961) showed the least scatter [curve 9], with a value of almost 0.3.

TABLE 4.2 STROUHAL NUMBER VERSUS REYNOLDS NUMBER

Curve #	Authors	Low Re	High Re	Medium	Comments
1	Lehnert (1937) (compiled data)	5.0E+01	2.0E+04	air	from Y. N. Chen paper
2	Drescher (1956)	1.5E+04	3.0E+05	air	
3	Haya - Yassuda (1961)	1.0E+05	3.0E+05	air	average stationary values
4	Bearman (1969)	1.0E+05	1.0E+06	air	group #2, wake measurements
5	Relf - Simmons (1924)	1.0E+05	8.0E+05	air	group #1, wake measurements
6	Ribner - Etkins (1958)	4.0E+04	3.0E+05	air	wake measurements
7	Davenport (1959) (compiled data)	5.0E+06	2.0E+07	air	concrete cylinder, roughness = .0009
8	Wooton	8.0E+05	1.0E+07	air	uniform flow, smooth
9	Roshko (1961)	3.5E+06	9.0E+06	air	uniform flow, roughness = 0.0002, wake measurements
10	Delany - Sorensen (1953)	1.5E+06	2.0E+06	air	uniform flow, wake measurements
11	Atking (slightly rough)	1.5E+04	8.0E+06	air	slightly rough surface, strong vortex shedding
12	Rodenbusch et. al. (Shell, 1983)	1.6E+05	2.1E+06	water	smooth, uniform flow
13	Rodenbusch et. al. (Shell, 1983)	1.6E+05	1.9E+06	water	roughness = .02, uniform flow
14	Jones	1.0E+05	1.3E+06	air	smooth uniform flow, spectrum peak measurements
15	Macovsky (1958)	2.0E+04	9.0E+04	air	spectrum peak measurements
16	Fung (1960)	3.0E+05	1.1E+06	air	spectrum peak measurements
17	Coder (1972)	5.0E+05	1.3E+06	air	smooth, rms wake measurements
18	Fung (1960)	6.0E+05	1.2E+06	air	rms wake measurements (some values for oscillating cylinders)
19	Chen	3.0E+01	1.8E+05	air	from Y. N. Chen , smooth, low turbulence, theory
20	Chen	3.0E+01	1.0E+07	air	from Y. N. Chen , rough, high turbulence, experiments
21	Sallet	1.0E+02	1.0E+06	air	from "D. W. Sallet's Data", experimental
22	Davenport (1959) (compiled data)	1.4E+06	9.0E+06	air	metal cylinder, roughness = 0.009
23	Hanson	4.9E+01	1.4E+02	air	hot wire anemometer
	Nishioka - Sato	5.3E+01	1.5E+02	air	hot wire anemometer
	Gaster	5.3E+01	2.0E+02	water	hot wire anemometer, shedding from long, slender cone
24	Roshko	5.0E+01	1.4E+03	air	hot wire anemometer
25	Lugt - Haussling	2.0E+02	2.0E+02	-	calculation, flatplate = 45 degrees
26	Kovaznay	5.5E+01	7.5E+03	air	hot wire anemometer
27	Bishop - Hassan	3.6E+03	1.1E+04	water	strain gauge force measurements
28	Jones	3.0E+06	1.8E+07	air	uniform flow, pressure transducer, L/D = 5.3
29	Jordan - Fromm	1.0E+02	1.0E+03	-	calculation
30	Achenbach - Heinecke	2.0E+04	5.0E+06	air	smooth, uniform flow
31	Schewe (1983)	2.3E+04	7.1E+06	air	smooth uniform flow

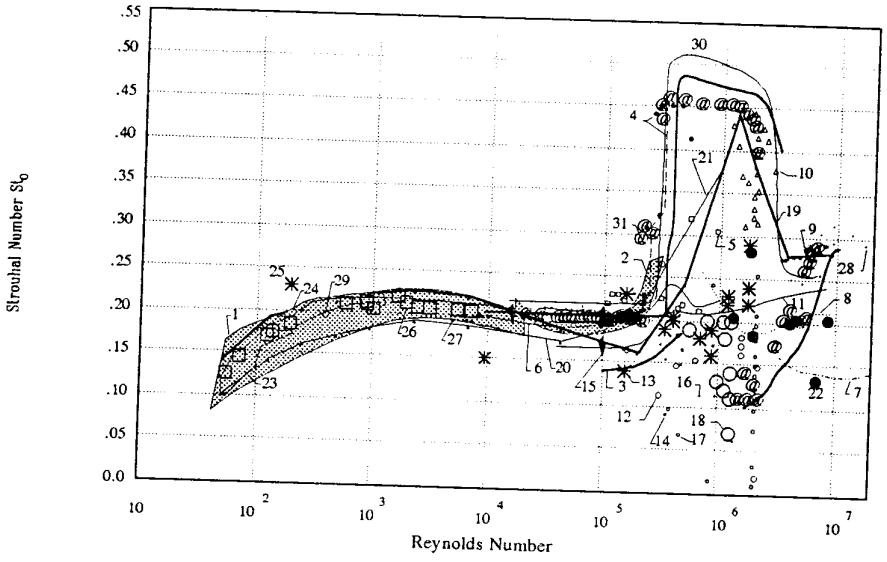

FIGURE 4.7 STROUHAL NUMBER VERSUS REYNOLDS NUMBER

4.2.2 *Bandwidth*

The lift force power spectrum can be used to illustrate the frequency content of the shedding process. Representative power spectra of the unsteady lift force as a function of Reynolds number are included in Figure 4.8 for a smooth, stationary cylinder in uniform flow. In the subcritical flow regime the unsteady lift spectrum is fairly narrow band, with a center Strouhal number (at the spectral peak) of about 0.2. In the transitional regime the peak lift frequency can shift dramatically to higher Strouhal values between 0.4 and 0.5. Higher values seem to be associated with lower turbulence of the incident flow. The lift spectrum then widens and the peak Strouhal frequency reduces below 0.2. Multiple peaks occur in the lift spectrum for supercritical flow. Strouhal numbers of the largest peaks remain below 0.2 in the supercritical regime for Reynolds number below about $2x10^6$. Above this Reynolds number, the Strouhal numbers of the major peaks gradually increase from about 0.2 towards 0.3 as the postcritical regime is approached. In the postcritical flow regime the Strouhal number is singled valued (as in the subcritical) with a Strouhal number about 0.3.

Intuitively one would expect that bandwidth (standard deviation of the shedding frequency as called alternatively) of the independent force should be based on turbulence and on slope of the current profile, but there is presently little guidance on either in the literature. Limited observations of force spectra in a wind tunnel [Vickery et. al. (1972) and Novak et. al. (1975)] have shown significant variations of the bandwidth parameters at different values of turbulence intensity.

Nevertheless, if the incident flow contains relatively large fluctuations in velocity (i.e. relatively high values of turbulence intensity), then the bandwidth will have a high value. High turbulence intensity will probably cause oscillation amplitudes to be sufficiently small, lock-in not to occur, and the response to be characterized by a broad-band spectrum. If there is no turbulence the force spectrum will have a very narrow band.

Highly sheared profiles will result in broad force spectra, due to the overlapping of adjacent cells shedding at different frequencies. The shear adjustment should be based on typical vortex cell lengths and overlap of adjacent cells at different frequencies, as described in Section 4.2.3. As this is a new concept, a suitable relationship will have to be developed.

Only a few studies were found that address the effect of flow characteristics on the bandwidth [Vandiver (1988)]. Reynolds and Keulegan-Carpenter numbers influence the shedding process, affecting the mean and distribution characteristics of the local shedding frequency. However, no data exists to relate these parameters to the bandwidth.

Vandiver (1988) used closed-form expressions for the standard deviation based on turbulence of the current velocity: B = T*fs, where B is the bandwidth, T is the percentage of turbulence in the flow, and fs is the shedding frequency. Typical turbulence intensity values of 0.1 to 0.2 (turbulence is 10 to 20% of the maximum current in the profile) have been suggested in the literature.

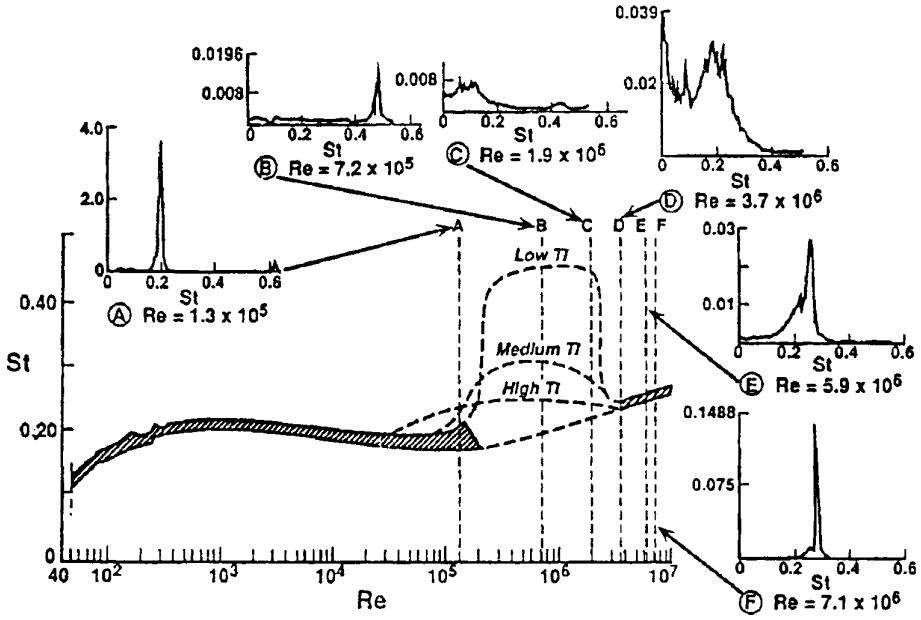

FIGURE 4.8 POWER SPECTRUM OF LIFT FORCE (SHEPPARD ET. AL. 1992)

4.2.3 Vortex Cells

Experimental evidence from uniform and shear flows about stationary cylinders indicates that the shed vortices have a significant length in the axial (along the cylinder axis) direction, leading to the term "vortex cell". Smoke visualizations of shear flow about a cylinder have shown shed vortices swept downstream at an angle to the incident flow, indicating spanwise correlation of vortex cell detachment [Stansby (1976)].

Figure 4.10 presents wake velocity power spectra taken from locations along the axis of a stationary cylinder in shear flow. If vortices were being shed everywhere according to the local Strouhal number, the peak frequencies on the figure would lie along an inclined line associated with the shear velocity profile. Instead, note the two regions of the cylinder marked by a vertical bar (added to the reproduction of the original figure) near the cylinder ends. These illustrate regions of nearly constant shedding frequency, indicating persistent cells of three-dimensional vortices being shed. There seems to be a transition area in the middle where cells of vortices shed at different frequencies overlap, leading to lower, wider spectral peaks.

It is likely that the added organization of vortex shedding indicated by persistent cells at the cylinder ends are an artifact of the test itself, in that the presence of cylinder ends (and associated end plates) somewhat inhibits axial movement of vortex cells being shed. In other words, the so-called "transition" area mentioned above may be most representative of shedding on a very long cylinder, except very near the ends. Therefore, although vortices shed themselves in cells, the spanwise location of these cells varies randomly in time. It seems reasonable to assume that correlation between cells is relatively low, which is consistent with the idea that the spanwise correlation of lift force is generally low for stationary cylinders, and that correlation length of the lift force can be shorter than the length of typical vortex cells (see subsequent section on correlation length). It also suggests that the frequency content of lift force is a function of the slope of the incident velocity profile, with more highly sheared flow leading to a wider bandwidth due to the overlap of cells being shed at different frequencies.

4.3 Correlation Length

The degree of correlation between lift forces along the cylinder axis is a key factor in determining net force, and therefore, vibration amplitude. Correlation is often computed for lift pressure or wake velocity measurements along a cylinder. High correlations indicate a strong relationship between the measurements, typically leading to increased lift over the section between measurement points.

Correlation length is a derived parameter, and as such is subject to a variety of interpretations. The correlation length may be defined simply as the integral of the correlation coefficient (Bearman, 1984):

$$L(z_1) = \int_{z_1}^{\infty} \rho(z_1, z)\,dz$$

Thus correlation length can be interpreted (somewhat loosely) as a distance over which the underlying variables are correlated. It is commonly quantified as a multiple of cylinder diameter.

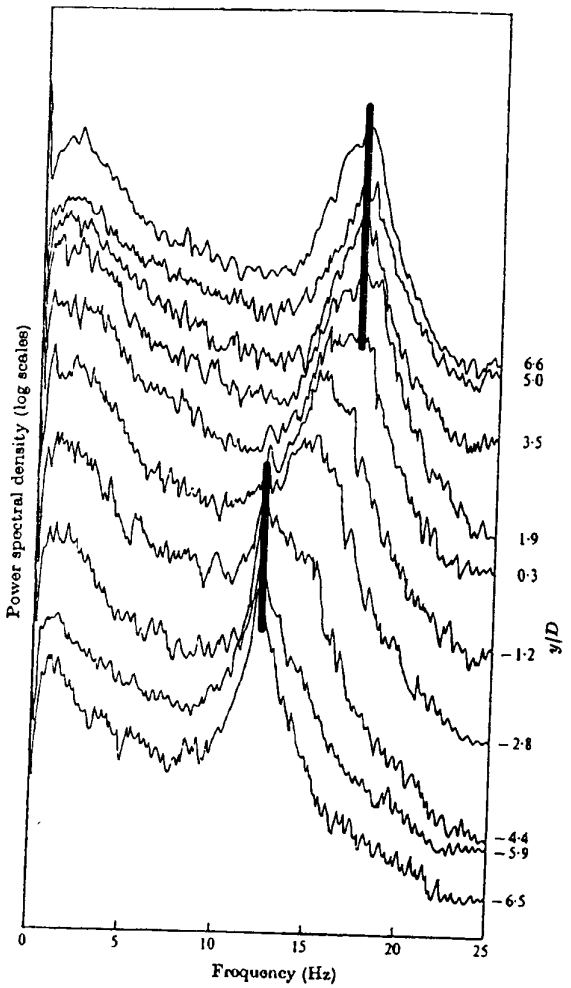

FIGURE 4.10 POWER SPECTRUM OF WAKE VELOCITY FOR SHEAR FLOW (STANSBY 1976)

The most frequently used method to derive correlation length involves velocity, pressure, or force measurements at two or more locations along a cylinder length.

Correlation coefficients are calculated as a function of the separation distance between the various locations. Closed form curves are then used to approximate correlation coefficient functions with respect to separation distance. Integration of the correlation coefficient function with respect to a separation distance between two locations (points 1 and 2) results in a correlation length at the reference location (e.g. point 1).

Longer correlation lengths lead to larger total force [Bendat & Piersol (1986)] and therefore generally larger response. Variations in correlation length affect lift coefficient values reported from lift force experiments. Researchers whose test setup or technique lead to shorter correlation lengths will report lower values of lift. Therefore, it is essential that correlation length be accounted for, implicitly or explicitly, in both interpreting the lift coefficient data as well as developing predictive models.

Some researchers have attempted to measure correlation length, and have developed data that shows some variation with Reynolds number, and a high sensitivity to oscillation amplitude. The following sections discuss these data and present the results.

4.3.1 Reynolds Number Dependence

Several studies were found that address the variation of correlation length with Reynolds number for stationary cylinders. For stationary cylinders it appears that correlation length is between one and six diameters for Reynolds numbers between 10^2 and 10^8 .

Compiled data, from stationary cylinders, of correlation length as a function of Reynolds number are presented in Figure 4.12. Related information about each model test are presented in Table 4.4. The majority of the model tests were performed in a wind tunnel under uniform flow conditions. The subcritical flow region was the most frequently studied, although several tests were performed in the transcritical and postcritical region.

King (1977), in compiling results of stationary smooth cylinders in uniform flows, found that the correlation length is high in the laminar boundary layer region (Re<150), and has a relatively high value in the subcritical region. The correlation length decreases to small values in the critical and supercritical regions where the flow is non-regular and random, and then increases slightly in the postcritical region where some regularity in the vortex shedding process re-appears. Thus, King reported that Gerlach et. al. (1970), [curve 1], found correlation lengths up to 20D, (where D is cylinder diameter) for Re<150, 2D-3D for Re<10^5, and 0.5D for Re>10^5. El Baroudi (1960), [curve 2], measured correlation lengths of 3D-6D in the subcritical region for circular smooth cylinders in uniform flow. Humphreys (1960), [point 3], found that the correlation length was about 1.5D in the critical/supercritical region.

Chen (1972) compiled correlation length data for stationary cylinders in wind under uniform flow [curves 5, 6, 7]. Experiments by Prendergast (1958), [curve 5] showed a maximum correlation length of 4D in the subcritical region and a drop to 0.5D in the critical region. Subcritical model tests by Etkin et. al. (1958), [curve 7], produced a constant correlation length of 8D. Results of model tests by Schmidt (1965), [curve 6], in the critical and supercritical region, showed very small correlation lengths of 0.4D.

Dronkers et. al. (1976), [curve 4], who performed model tests with stationary cylinders in water under uniform flow for Reynolds numbers between 10^3 - 10^5 (subcritical region), observed an abrupt change in correlation length at Re=$1.6x10^4$, from 3.8D to 7.9D. He could not provide any explanation for this change. Note that lift coefficient attains its maximum value for stationary cylinders in uniform flow at Reynolds numbers between $2x10^4$ - 10^5. This is not coincidental. High correlation length will result in higher lift force, leading to increased lift coefficients reported for this Reynolds number region.

Szechenyi (1975), in supercritical tests for smooth cylinders and postcritical tests for a roughened cylinder, found extreme scatter in the results for supercritical flow such that only a mean value could be derived. Extrapolation of his results produced correlation lengths of 1D and 9D, respectively, for supercritical and postcritical regimes. Szechenyi's correlation length data in the supercritical region agree with values estimated by other researchers. However, the high correlation length of 9D in the postcritical region for roughened cylinders, along with the high scatter he noted, makes this correlation length value questionable.

Bearman (1984), suggested that the correlation length for a circular cylinder varies between 3 and 6 diameters for the range of Reynolds numbers 10^4 - 10^5. He argued that although the mutual interaction between two shear layers, which leads to the generation of regular vortex shedding, may be very strong in the subcritical region, spanwise coupling appears comparatively weak. Bearman's suggestions are within the range of correlation lengths shown in Figure 4.11.

Blevins (1986) in compiling data for stationary cylinders, found typical correlation length values ranging from 100 or more diameters for laminar vortex streets at Re=60, to 20 diameters at Re=100, and 5 diameters for fully turbulent vortex streets at Re=10^4. Blevins also noted that when the free stream flow velocity varies over cylinder span (shear effect), these cells also develop but the shedding frequency is not constant but varies discretely in ladderlike steps along the span with each step spanning about 4D. This is consistent with Stansby's data, discussed previously in Section 4.2.3.

TABLE 4.4 CORRELATION LENGTH DATA FOR STATIONARY CYLINDERS

Curve #	Authors	Low Re	High Re	Medium	Comments
1	Gerlach (1970)	4.0E+01	1.0E+05	air	uniform flow
2	El Baroudi (1960)	1.0E+04	4.5E+04	air	uniform flow
3	Humphreys (1960)	2.0E+05	2.0E+05	air	single point, uniform flow
4	Dronkers - Massie (1976)	1.0E+03	1.0E+05	water	uniform flow, fixed cylinder
5	Prendergast (1958)	2.0E+04	2.0E+05	air	uniform flow
6	Schmidt (1965-66)	1.5E+06	8.0E+06	air	uniform flow
7	Etkin - Keefe - Korbacher (1957)	2.0E+04	6.0E+04	air	uniform flow
8	Scruton (1957)	1.0E+04	7.0E+05	air	uniform flow

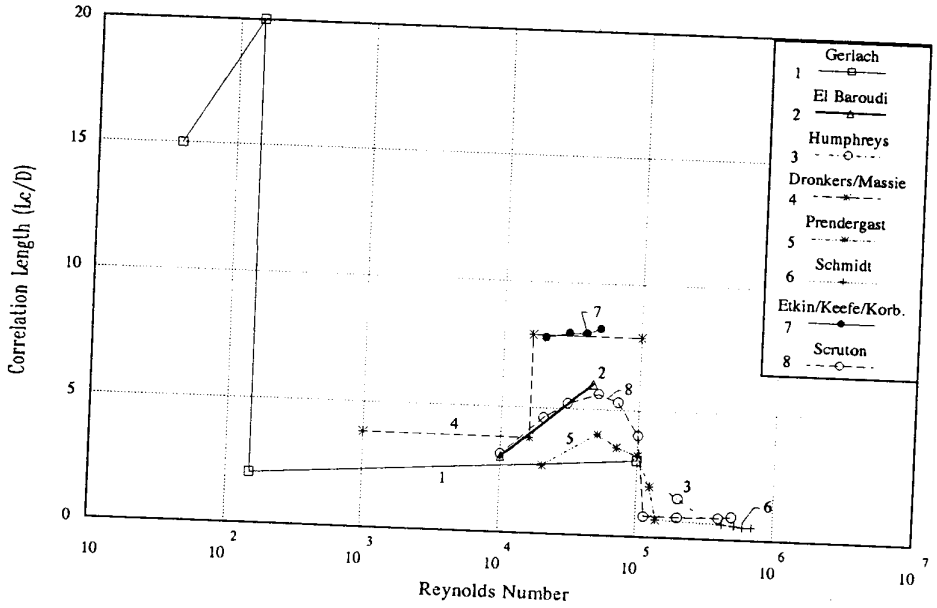

FIGURE 4.11 CORRELATION LENGTH FOR STATIONARY CYLINDERS

Some of the most careful model tests were performed by Howell et. al. (1980). The correlation coefficient was investigated as a function of location of the reference point (a stationary point on the cylinder where a pressure transducer was placed, while another pressure transducer was moved along the cylinder length). Howell noted that correlation for the stationary cylinder is very dependent on location of the reference point and the direction in which measurements are taken. The sensitivity noted by Howell was likely due to his test setup. Howell tested a cantilevered cylinder, L/D = 10, attached at the bottom to the tank floor and free at the top. Howell's measurements were therefore affected by two different types of end conditions. The implication of this observation is that is very difficult to obtain accurate correlation data for stationary cylinders, and that all such data in the literature should be scrutinized very carefully and understood thoroughly before using in a predictive model.

5.0 FLUID-STRUCTURE INTERACTION

Hydrodynamic forces on an oscillating cylinder are much more complex than lift on a stationary cylinder due to interaction between the oscillating cylinder and the fluid medium. In general, hydrodynamic force on an oscillating cylinder includes added mass and damping forces in

addition to lift. Furthermore, the lift force may be substantially different from that measured on an equivalent stationary cylinder.

Effects on lift force resulting from interaction include changes in lift force magnitude, frequency, and correlation length. These effects have been extensively researched, and a great deal of information is available from a variety of tests on spring-mounted, flexible, and oscillated cylinders in both air and water. In general, the fundamental fluid behavior that determines force magnitude, frequency, and correlation is similar in all cases. However, interpretation of data from different types of tests requires great care.

For example, it is generally accepted that added mass and damping forces generated by cylinder motion are important in water but insignificant in air. Added mass in air is very small relative to cylinder mass for typical engineering structures, and therefore contributes little to overall response of the system. At resonance in water, lift forces on cables and risers are generally equilibrated by hydrodynamic damping, meaning that damping force generated on a cylinder in water is of the same magnitude as lift force. For cylinders resonating in air, aerodynamic damping is generally very small[1], and damping provided by the material or supports is more important. This suggests that data developed in air will predominately reflect applied lift force, while data developed in water will contain significant components of hydrodynamic added mass and damping. However, there are also problems unique to data in air that affect lift coefficients developed in the wind tunnel. These issues are discussed in more detail in the following sections.

5.1 Lift Force Magnitude

In order to utilize oscillating cylinder data from the literature, it is essential to understand not only how the hydrodynamic force was measured, but also how various force components were defined and identified. Many experiments have been conducted in which the cylinder freely oscillated in response to applied forces. Examples include the data from Weaver (1961), Feng (1968), and Cheung and Melbourne (1980). In some cases only cylinder amplitude is measured, as the research was focused on identifying maximum amplitudes as a function of various modeling parameters like reduced velocity, mass, and damping. In other cases, hydrodynamic force amplitude was measured and used to compute a "lift" coefficient, yet the reported coefficient may implicitly contain the effect of hydrodynamic damping and added mass. It is essential to fully understand this aspect of oscillating cylinder data, so that damping and added mass forces are not misinterpreted as excitation force.

[1]This can be seen by comparing lift to damping at typical wind speeds and vibration amplitudes. In air, wind velocity is typically much greater than structural velocity, and therefore lift dominates aerodynamic damping.

Extensive data has also been gathered via oscillated cylinder experiments where the cylinder is forced to oscillate in a steady flow at a prescribed frequency and amplitude. Hartlen et. al. (1970), and Sarpkaya (1977) assumed a harmonic function for total hydrodynamic force and split it into two components: one in phase with cylinder velocity, and one 180° out of phase with cylinder acceleration. This approach completely describes the amplitude and phase (relative to the prescribed displacement) of a linear force. The former (called hydrodynamic damping) will add or subtract energy to the vibrating cylinder, while the latter (called added mass) will perform no net work over one cycle. The regular forces are determined by averaging over long time intervals. This force formulation is equivalent to a Morison approximation for wave forces.

Other researchers have also approximated the force on an oscillated cylinder as being harmonic. Bearman (1984), and Rajabi et. al. (1983) observed that this was an acceptable assumption in model tests where the cylinder vibrates in lock-in conditions. Note, however, that "lift" as an excitation force is not explicitly separated from forces due to cylinder motion. A different example is Griffin (1981), who splits the hydrodynamic force in three components: added mass, damping, and lift force. In this case, some arbitrary partitioning of the force is necessary, as there are only two independent variables (amplitude and phase).

5.1.1 Oscillating Cylinders in Air

Data on oscillating cylinders tested in air are compiled in Figure 5.1. Curve 13 was derived from pressure measurements, while curves 7, 8, and 45 were compiled from force measurements. Descriptions of the experiments are summarized in Table 5.1.

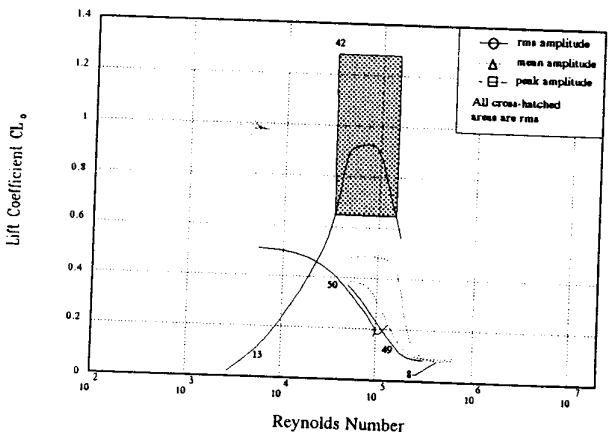

FIGURE 5.1 LIFT COEFFICIENT FOR OSCILLATING CYLINDER (IN AIR)

TABLE 5.1 LIFT COEFFICIENT DATA FOR OSCILLATING CYLINDERS

Curve #	Authors	Low Re	High Re	Medium	Value	Comments
7	Cheung/Melbourne (1983)	6.0E+04	7.0E+05	air	mean peak	Iu=1.6%, uniform flow, elastically-mounted cylinders, L/D=3.6-6.7
8	Cheung/Melbourne (1983)	6.0E+04	7.0E+05	air	mean peak	Iu=0.4%, uniform flow, elastically-mounted cylinders, L/D=3.6-6.7
13	Gerrard (1961)	5.0E+03	1.8E+05	air	rms	Iu=0.3%, pressure measurements, L/D=6.6-80
42	Vickery/Watkins (1962)	4.0E+04	1.8E+05	air/water	rms	Stationary and oscillating cylinder data, (also Table 5.1)
44	Warren (1962)	1.2E+04	9.0E+04	water	mean peak	uniform flow
48	Bishop/Hassan (1964)	4.0E+03	1.2E+04	water	mean peak	uniform flow, rigidly-mounted, forced vibrations, strain gages, A/D=0.3
49	Weaver (1961)	8.0E+04	4.0E+05	air	rms	elastically-mounted cyl, Iu=0.5%, unif. flow, force measurements, L/D=20
50	Weaver (1961)	8.0E+03	1.0E+05	air	rms	self-excited cyl, Iu=0.5%, uniform flow, force measurements, L/D=20-40

Gerrard (1961), [curve 13], placed cylinders with aspect ratios 6.6 to 80 in a wind tunnel under uniform flow with a turbulence intensity of 0.3%. Gerrard did not oscillate his test cylinders at a prescribed amplitude and frequency. He observed that the cylinder vibrated independently of the boundary conditions. Gerrard's rms lift coefficient was derived from pressure measurements, and has a maximum value of 0.92 at Reynolds number about $9x10^4$. The lift decreases for Reynolds numbers $>10^5$. Gerrard's curve is a best-fit to the data.

Curves 7 and 8, Cheung & Melbourne (1983), were derived from wind tunnel tests using spring-supported rigid cylinders of aspect ratios 3-6 and end plates, for subcritical and transitional flow conditions, and for several turbulence intensity values between 0.4-9.1%. They measured in-line and transverse forces at the cylinder end-points. Lift force was probably correlated because the aspect ratio were less than 6 (Section 4.3). Cheung et. al. corrected the lift force measurements for blockage effects.

Cheung et. al. observed that as the organized shedding disappears in the critical flow regime, the fluctuating lift drops to a lower value and becomes relatively constant up to the supercritical flow regime. In the presence of turbulence, the decrease in fluctuating lift in the critical flow regime is shown to occur at a lower Reynolds number. In addition, the fluctuating lift seems to decrease with increasing turbulence values at subcritical Reynolds numbers. It seems reasonable to assume that turbulence might reduce both correlation length and the strength of vortices shed in the upper subcritical regime. In the supercritical flow regime, on the other hand, the increased entrainment due to turbulence could reduce the vorticity in the free shear layers and cause the wake to fluctuate more, effectively broadening the wake. The swinging of the wake, in effect, induces a slight *increase* in the fluctuating lift [Cheung et. al. (1983)].

Lift coefficients derived for low turbulence intensities of 0.4% and 1.6% are represented by curves 8, and 7, respectively. These curves follow the general lift coefficient characteristics of high lift in the subcritical regime, a drop in the critical regime and low constant lift in the supercritical regime. Maximum mean amplitude values are 0.5 and 0.4 for the 0.4% and 1.6% turbulence intensity, respectively. Two points are of interest here: 1) The effect that turbulent intensity has on the lift coefficient in wind tunnel tests, and 2) Turbulence intensity of 1.6% is not considered high turbulence for practical applications. It is possible that lift coefficients in the subcritical regimes will be lower, and lift coefficients in the supercritical regimes will be higher, at typical open air or ocean turbulence intensities of 2%-5%.

Cross-hatched area 42 includes stationary & oscillating cylinder data. The substantial scatter in the lift coefficient is expected due to correlation and other effects as discussed in section 4.1.1. Curves 49, and 50 [Weaver (1961)] represent rms lift coefficient data from elastically-mounted and vibrating members with various end connections (fixed, partly-fixed, pinned, cantilever), respectively, using relatively flexible cylinders with aspect ratios between 20-40. The curves cover Reynolds numbers from $8x10^3$-$4x10^5$. The lift coefficients were corrected for blockage effects. Weaver estimated that the lift force amplification with respect to the stationary cylinder was 1.1-1.2 on the average. The amplification factors were higher for the elastically-mounted cylinders than for the flexible members. These lift coefficients appear low for oscillating cylinders, possibly because vibration amplitudes were low (maximum of .13 A/D). The high aspect ratio of the cylinders, combined with relatively low vibration amplitudes, would tend to keep correlation low and thus limit the total measured force. In addition, some small roughness may have shifted the flow characteristics to occur at a lower Reynolds number, as can be concluded by comparing curves 49 and 50 to curves 7 and 8.

5.1.2 Oscillating Cylinders in Water

Data from the literature on oscillating cylinders tested in water are compiled in Table 5.1 and Figure 5.2. The data

by Bishop et. al. (1964), [curve 48] forced-oscillations of rigidly-mounted short cylinders, showed a high drop of the lift coefficient in a relatively small Reynolds number range, $4x10^3$-$1.1x10^4$. Their data represent mean amplitude values obtained from oscillating cylinders at a prescribed amplitude and frequency in flowing water. Hydrodynamic force was measured by force transducers, and inertial, added mass, and damping forces obtained from oscillating the same cylinder in still water were subtracted. The result is an approximation of the lift force.

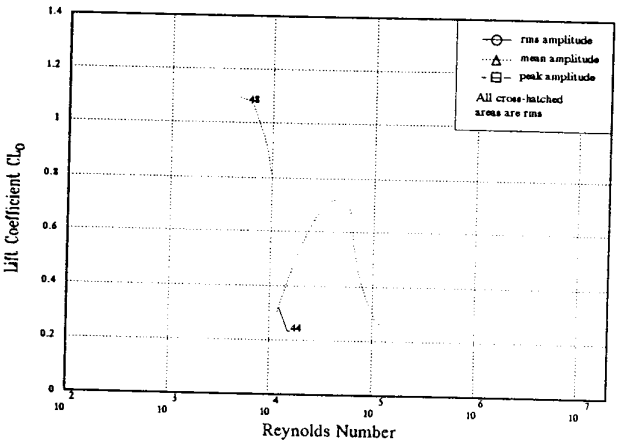

FIGURE 5.2 LIFT COEFFICIENT FOR OSCILLATING CYLINDER (IN WATER)

In their paper, however, there is no mention of correlation effects on the measurements. It is reasonable to assume, however, that the lift force was fully correlated in their tests. Curve 48 refers to mean amplitude lift coefficient for response amplitude A/D=0.3 (A=amplitude, D=diameter), at an oscillation frequency equal to the vortex shedding frequency of an equivalent stationary cylinder. The curve was derived from nondimensional vibrating and stationary cylinder test data found in Bishop's paper, coupled with stationary cylinder data from Bishop reported in other references.

Curve 44 [Warren (1962)] was obtained from Sarpkaya's compiled data [Sarpkaya (1981)]. The curve represents measured lift forces on a self-excited cylinder in uniform flow. Data on the magnitude of the amplitude, and the frequency of the vibration, are not available. Nevertheless, Warren's curve follows the expected lift coefficient behavior with peak amplitude of 0.7 at Reynolds number of 5×10^4.

5.1.3 Amplitude Dependence

A compilation of published data demonstrating amplitude dependence is presented in Figure 5.3. These data were collected from individual studies and from other compiled data review studies [Blevins (1986), Griffin (1981)]. A few lift coefficient values reported in the literature were derived from analytical studies based on experimental results [Blevins et. al. (1976)]. Related information about each model test is summarized in Table 5.2.

Amplification of lift force due to synchronization of vortex shedding and cylinder motion has been demonstrated for subcritical flow. Available test data were derived from spring-mounted, oscillated, and flexible cylinder model tests in the subcritical flow region. However, no model tests were located in the transitional or postcritical regions, making it difficult to draw firm conclusions for these Reynolds number ranges. In addition, the reader is reminded that these data must be interpreted subject to all of the same concerns raised earlier about lift coefficients for moving cylinders. In other words, where the reported data show an increase in lift coefficient, the reader must consider this first as an increase in net hydrodynamic force, and attribute the increase appropriately to changes in lift force coefficient, correlation length, and other factors relevant to a particular predictive model.

Some important characteristics of the unsteady lift and pressure forces that accompany vortex-induced oscillations are clear from the compiled data. First, there is a maximum of the excitation force at a peak response amplitude between 0.4 to 0.6 diameters. Second, the maximum of the force coefficient is approximately C_L=0.5 to 0.6 for all cases except two: curve 5 with maximum lift coefficient value about 0.75 [Sarpkaya (1979)] and curve 16 with value about 1.2 [Bishop et. al (1964)]. Values reported for C_L then decrease towards zero in all cases, presumably resulting in a response amplitude limited to 1 - 2 diameters.

Bishop's experiments represent the first complete set of tests to document the effect of vibration amplitude on lift force [Bishop et. al. (1964)]. Bishop's data are mean amplitude values obtained from cylinders oscillated while under tow in a water flume. For constant response amplitude of 30% of diameter they showed C_L to decrease from 1.0 to 0.8 as Reynolds number increased from $6x10^3$ to $9.9x10^3$. At constant $Re=6x10^3$, C_L increased from 0.7 to 1.2 as response amplitude increased from 0.2 to 0.4. In their paper, however, there is no mention of correlation effects on the measurements, as well as of the other parameters that would affect lift force (blockage, turbulence etc.).

TABLE 5.2 AMPLITUDE DEPENDENCE OF LIFT COEFFICIENT

Curve #	Authors	Low A/D	High A/D	Medium	Value	Comments
1	Hartlen et al. (1968)	8.0E-02	1.5E-01	air	peak	cantilever beam, L/D = 13.8, flexible, aluminum pipe
2	Walshe Data (1962)	0.0E+00	1.0E-01	air	peak	L/D = 7.8, Re = 1.2E5
3	Vickery - Watkins (1964)	5.0E-02	7.0E-01	water/air	peak	cantilever beam, L/D = 15
4	King (1977)	1.0E-01	1.6E+00	water	peak	flex. and cantilever, PVC, Al, and S. Steel, avg. per Vickery/ Watkins
5	Sarpkaya (1978)	1.0E-01	1.0E+00	water	peak	aluminum tubing, rigid cyl, forced oscillations
6	Vickery - Watkins (1964)	9.5E-01	1.5E+00	water/air	peak	cantilever beam, L/D = 48
7	Griffin - Koopman (1977)	1.0E-01	7.0E-01	air	peak	spring-mounted rigid cyl, aluminum-tubing
8	Vickery - Watkins (1964)	0.0E+00	1.3E+00	water/air	peak	brass, pivoted rigid cylinder
9	Blevins (1976)	0.0E+00	1.4E+00	water/air	peak	H/D = 48 (theory)
10	Blevins (1976)	0.0E+00	1.4E+00	water/air	peak	H/D = 15 (theory)
11	Mercier (1973)	3.0E-01	1.2E+01	water	peak	stainless steel, forced oscillations
12	Wake Oscillator Theory Model	0.0E+00	1.6E+00	air	peak	H/D = 13.8, flexible
13	Vickery-Watkins (1962)	2.0E-01	1.4E+00	water/air	peak	stainless steel, forced oscillating model
14	Vickery-Watkins (1962)	0.0E+00	1.5E+00	water/air	peak	brass, forced oscillating model
15	Vickery-Watkins (1962)	2.0E-01	2.1E+00	water/air	peak	PVC, forced oscillating model
16	Bishop & Hassan (1963)	2.0E-01	4.0E-01	water	peak	strain gage measurements, forced oscillations
17	Tanida et al (1973)	1.4E-01	1.4E-01	-----	peak	oscillating cylinder uniform flow
18	Wang et al (1986)	0.0E+00	4.0E-01	-----	peak	theory/compilation, for oscillated cylinder
19	Howell et al (1980)	0.0E+00	1.0E-01	air	rms	strain gage measurements, oscillated cylinder

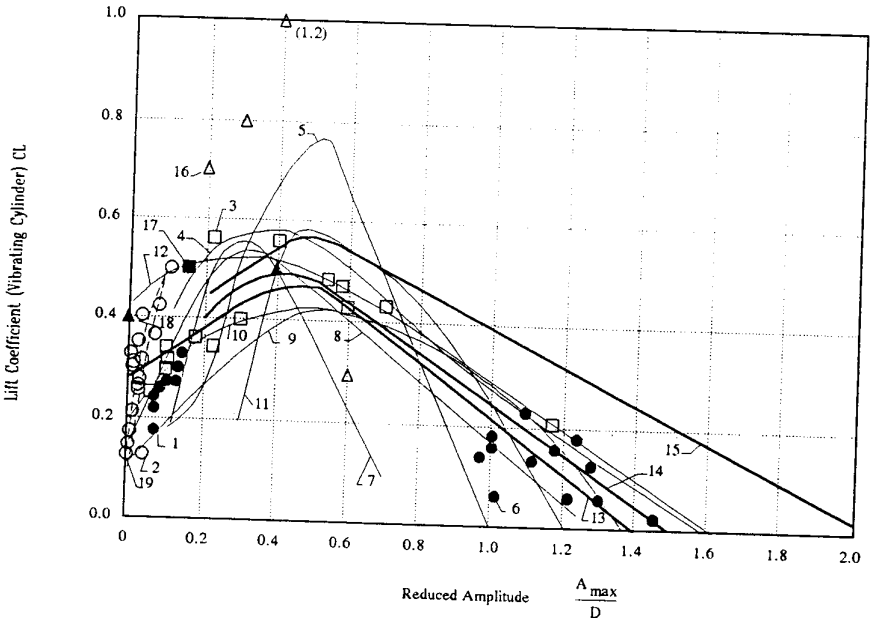

FIGURE 5.3 AMPLITUDE DEPENDENCE OF LIFT COEFFICIENT

Experiments similar to those conducted by Vickery et. al. (1962) were performed by Diana et. al. (1971). Measurements of lift forces on a spring-mounted cylinder freely vibrating in a wind tunnel showed that lift forces reached a maximum value at response amplitudes about 50 - 60% of diameter, beyond which lift began to decrease as the vibration amplitude increased further. A limiting amplitude of vortex-induced oscillation equal to 100% of diameter was computed by Diana & Falco, thus confirming the earlier finding of Vickery and Watkins.

Griffin et. al. (1977), [curve 7], and also Skop et. al. (1973), investigated the dependence of the lift coefficient on the vibration amplitude in the subcritical range for the lock-in case. In their tests, amplification of about two times the value of lift from stationary cylinder tests was observed at amplitudes near 50% of diameter.

Wang et. al. (1986), [curve 18], defined the lift as the component of force in-phase with transverse cylinder velocity. They found that lift coefficient increased from about 0.4 at zero response amplitude to about 0.5 at response amplitude of 40% of diameter, and then decreased to zero at response amplitude of 150% of diameter.

Forced-vibrations model test results by Howell et. al. (1980), for circular cylinders in smooth flow in a wind tunnel, show a continuous increase to the lift force coefficient with amplitude up to 10% of diameter. The rms value of the local lift coefficient was 0.489 at a response amplitude of 10% of diameter. Their data are consistent with other data reported at the same Reynolds number of 7.5×10^4.

It is clear from the data that cylinder motion has an effect on lift force. There is a consensus in the literature, supported by the data, that lift increases with response amplitude up to a point, then decreases with further increases in amplitude. What is not clear is the mechanism behind this apparent dependence of lift on response amplitude. One possible mechanism is the increase in relative velocity between the moving cylinder and fluid. Higher relative velocity generates more transverse pressure behind the most recently shed vortice, resulting in a corresponding increase in lift force. While this may account for some increase in lift, it is unlikely to explain the large increase usually apparent at relatively moderate (10 to 50% of diameter) displacement amplitudes.

Another plausible mechanism is increased spatial correlation of the force. Cylinder motion organizes the wake and seems to increase spanwise correlation of vortex shedding process. The data suggest a minimum vibration amplitude for this process, which is typically called the threshold amplitude [King (1977)]. The threshold amplitude for cross-flow oscillations appears to be about 10% of a diameter. As the cylinder amplitude increases beyond approximately 50% of diameter, the cylinder begins to outrun the shedding vortices and the lift force begins to decrease [Blevins et. al. (1976)]. Large amplitude oscillations beyond 100 to 150% of diameter produce a breakdown in the regular vortex street, and the lift force diminishes rapidly.

Another potential mechanism is an increase in the integrated pressure force through variation in the separation points due to cylinder oscillation. Significant variation in location of the separation points has been observed experimentally in oscillated cylinder tests [Toebes (1969)]. It is possible that the corresponding change in pressure distribution (in particular, the area over which pressure is distributed) causes increased lift. However, it should be noted that the above mechanisms are not independent but are related because they are part of the fluid-structure interaction.

5.2 Lift Force Frequency

It is generally accepted that cylinder motion plays a critical role in determining the frequency content of lift force. Unfortunately, frequency content and related behavior of lift for oscillating cylinders is more difficult to study than that for stationary cylinders, and therefore the data are less extensive and the evidence is less conclusive. Furthermore, as discussed previously, researchers have not been consistent with their definitions of lift force for oscillating cylinders, making the literature difficult to interpret. However, there are several well-established phenomena related to the frequency characteristics of lift on oscillating cylinders that are important to the development of a predictive model. This section will discuss several important aspects of interaction between cylinder motion and lift force frequency, such as synchronization (lock-in) of lift, and general frequency/phase behavior of lift force on an oscillating cylinder.

5.2.1 Lock-In

Dramatic evidence of how cylinder motion can affect vortex cell formation, and therefore change correlation and shedding frequency, is illustrated in Figure 5.4. Each data point represents a peak frequency from a wake velocity power spectra. These data are plotted versus the Strouhal number of the incident flow measured at the middle of the shear velocity profile[2]. The lines connecting the data highlight the differences between vortex cells formed in the wakes of stationary (Figure 5.4a) and oscillating (Figure 5.4b) cylinders. Note that the change in behavior is striking for a cylinder oscillated at a Strouhal frequency of 0.198, despite the relatively small oscillation amplitude (0.06 diameters).

Clearly, cylinder motion has organized the shedding into distinct cells, the longest of which is synchronized with the cylinder motion. Thus, even relatively small cylinder motion at or near the nominal frequencies associated with vortex shedding organizes the shedding into distinct cells, like those observed at the ends of stationary cylinders. Similar data for cylinders oscillated at frequencies markedly different from the shedding frequencies indicate that the effect on cell formation is minimal. Data in Figure 5.5 are virtually the same as the stationary case, despite the higher amplitude (0.2 diameters).

Therefore it is clear that significant organization of the wake structure into correlated cells can occur when a periodic motion is applied to the cylinder. This wake

[2]This definition tends to obscure the fact that each vortex cell sheds at approximately the same Strouhal number relative to the local value of incident velocity. For example, the local velocity at y/d = 6 is 15% higher than that at y/d = 0 due to the shear flow. The "Strouhal" number in Figure 5.4 at y/d = 6 (0.23), when scaled by the ratio of velocity at y/d = 6 to velocity at y/d = 0 (1.15), is actually equal to 0.20.

organization can affect frequency content and spanwise correlation of the lift force. The data also suggest that this phenomenon is frequency-dependent, and will only occur for certain periodic motions of the cylinder at or near the shedding frequencies indicated for a stationary cylinder. Unfortunately, there is very limited data in the literature on non periodic cylinder motions, and therefore the organizing effect of narrow-band and wide-band random cylinder motions on wake structure remains rather speculative.

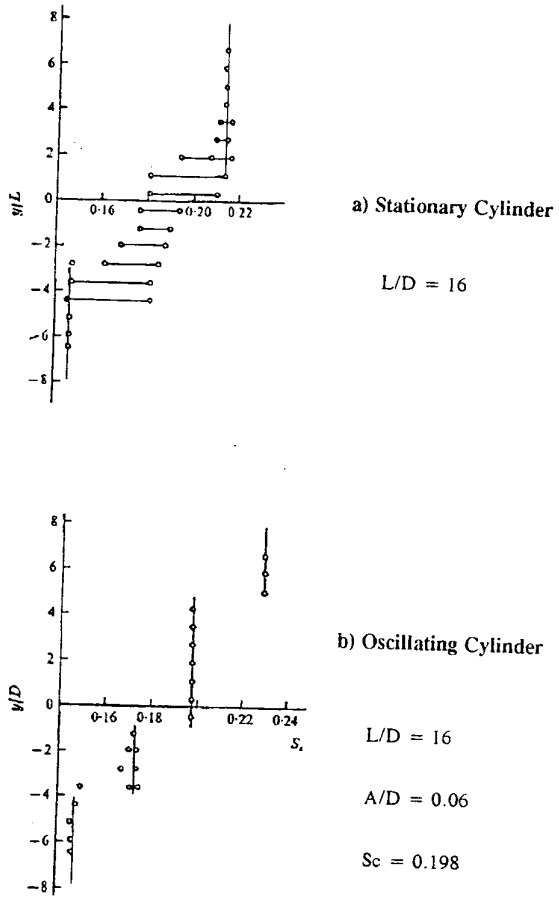

FIGURE 5.4 SPANWISE DISTRIBUTION OF SHEDDING FREQUENCY (STANSBY 1976)

These observations can be taken one step further by investigating the frequency characteristics of the wake as the frequency of cylinder motion is varied about the range of shedding frequencies. Figure 5.6 presents shedding frequency fs* versus cylinder oscillating frequency fc normalized by the shedding frequency of the stationary cylinder fo. The ordinate of each point is the ratio of shedding frequency of the oscillating cylinder to that of a stationary cylinder. Where the ordinate is 1.0, there is no difference. Where the ordinate is less than 1.0, shedding on the oscillating cylinder occurs at a lower frequency than that of a stationary cylinder under comparable flow conditions.

The slope of the line in Figure 5.6 represents change in shedding frequency with change in cylinder frequency. Note that the curve is generally flat (zero slope), but there are two areas with positive slope. The first occurs when the cylinder frequency is nearly equal to the nominal shedding frequency of a stationary cylinder (abscissa equal to 1.0), which as discussed above is an area characterized by significant organization of the wake into correlated, consistent vortex cells. The slope here is unity, indicating that the shedding frequency is equal to the cylinder frequency over a range of cylinder frequencies. The second occurs when the abscissa nears 2.0, with a slope of 0.33. In this range, the shedding frequency is equal to 1/3 of the cylinder frequency, over a range of cylinder frequencies.

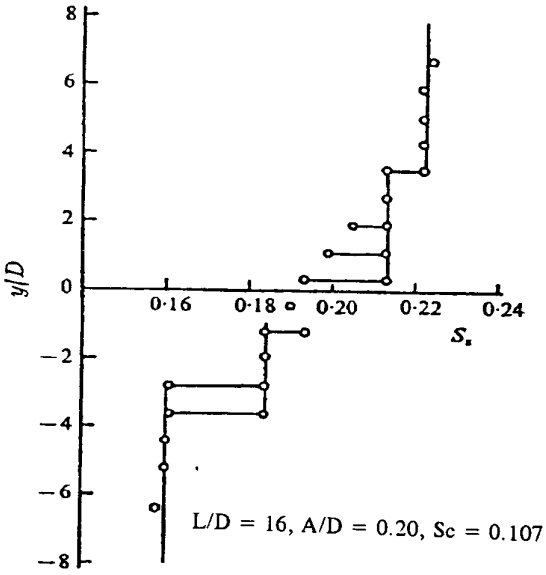

FIGURE 5.5 SPANWISE DISTRIBUTION OF SHEDDING FREQUENCY (STANSBY 1976)

The explanation for this behavior is that the motion of the cylinder organizes the wake and causes the shedding frequency to abruptly jump from its nominal value f_s to a value equal to the oscillation frequency f_c. At some point the shedding frequency reverts back to a constant frequency that is generally lower than that of a stationary cylinder. When the cylinder motion controls the shedding frequency in this way, the frequency is said to be locked-in, locked-on, or synchronized to the cylinder frequency, a phenomenon first reported by Bishop [Bishop and Hassan (1964)]. Note that shedding can be synchronized to the cylinder frequency f_c or subharmonics (e.g. $f_c/2$ or $f_c/3$).

* In Figure 5.6, frequencies are represented by their "equivalent" Strouhal number according to the relationship S = fD/V.